Jefferson Lab PAC14
Proposal Cover Sheet

This document must be received by close of business Thursday, **June 4, 1998** at:

Jefferson Lab
User Liaison Office,
Mail Stop 12B
12000 Jefferson Avenue
Newport News, VA
23606

Experimental Hall: C
Days Requested for Approval: 16

☑ **New Proposal Title:** Spin Polarization in Kaon Electroproduction
☐ **Update Experiment Number:**
☐ **Letter-of-Intent Title:**
(Choose one)

Proposal Physics Goals
Indicate any experiments that have physics goals similar to those in your proposal.

Approved, Conditionally Approved, and/or Deferred Experiment(s) or proposals:

PR 97-007 Conditionally Approved

Contact Person

Name: O. Keith Baker
Institution: Hampton University and Jefferson Lab
Address: Department of Physics
Address: Hampton University
City, State, ZIP/Country: Hampton, VA 23668
Phone: 757-269-7343 **Fax:** 757-269-7363
E-Mail: baker@jlab.org

Jefferson Lab Use Only

Receipt Date: 6/2/98 PR-98-[redacted] 101
By: gp

BEAM REQUIREMENTS LIST

JLab Proposal No.: 98-101 Date: 6/2/98

Hall: C Anticipated Run Date: _____ PAC Approved Days: _____

Spokesperson: D. Keith Baker Hall Liaison: Roger Carlini
Phone: 757-269-7343
E-mail: baker@jlab.org

List all combinations of anticipated targets and beam conditions required to execute the experiment. (This list will form the primary basis for the Radiation Safety Assesment Document (RSAD) calculations that must be performed for each experiment.)

Condition No.	Beam Energy (MeV)	Mean Beam Current (μA)	Polarization and Other Special Requirements (e.g., time structure)	Target Material (use multiple rows for complex targets — e.g., w/windows)	Material Thickness (mg/cm²)	Est. Beam-On Time for Cond. No. (hours)
1	4045	30	80% polarization	liquid hydrogen	standard	384

The beam energies, E_{Beam}, available are: $E_{Beam} = N \times E_{Linac}$ where N = 1, 2, 3, 4, or 5. E_{Linac} = 800 MeV, i.e., available E_{Beam} are 800, 1600, 2400, 3200, and 4000 MeV. Other energies should be arranged with the Hall Leader before listing.

HAZARD IDENTIFICATION CHECKLIST

JLab Proposal No.: 98-101 (For CEBAF User Liaison Office use only) Date: 6/2/98

Check all items for which there is an anticipated need.

Cryogenics
- ____ beamline magnets
- ____ analysis magnets
- ____ target
  - type: LH2
  - flow rate: ____
  - capacity: ____

Standard

Electrical Equipment
- ____ cryo/electrical devices
- ____ capacitor banks
- ____ high voltage
- ____ exposed equipment

standard

Radioactive/Hazardous Materials
List any radioactive or hazadorous/ toxic materials planned for use:

None

Pressure Vessels
- ____ inside diameter
- ____ operating pressure
- ____ window material
- ____ window thickness

Standard

Flammable Gas or Liquids
- type: ____
- flow rate: ____
- capacity: ____

Drift Chambers
- type: ____
- flow rate: ____
- capacity: ____

Standard

Other Target Materials
- ___ Beryllium (Be)
- ___ Lithium (Li)
- ___ Mercury (Hg)
- ___ Lead (Pb)
- ___ Tungsten (W)
- ___ Uranium (U)
- ✓ Other (list below)

empty target

Vacuum Vessels
- ____ inside diameter
- ____ operating pressure
- ____ window material
- ____ window thickness

Radioactive Sources
- ____ permanent installation
- ____ temporary use
- type: ____
- strength: ____

None

Large Mech. Structure/System
- ____ lifting devices
- ____ motion controllers
- ____ scaffolding or
- ____ elevated platforms

none

Lasers None
- type: ____
- wattage: ____
- class: ____

Installation:
- ____ permanent
- ____ temporary

Use:
- ____ calibration
- ____ alignment

Hazardous Materials
- ___ cyanide plating materials
- ___ scintillation oil (from)
- ___ PCBs
- ___ methane
- ___ TMAE
- ___ TEA
- ___ photographic developers
- ___ other (list below)

None

General:

Experiment Class:
- ✓ Base Equipment
- ____ Temp. Mod. to Base Equip.
- ____ Permanent Mod. to Base Equipment
- ____ Major New Apparatus

Other: ____

LAB RESOURCES LIST

JLab Proposal No.: 98-101 Date 6/2/98
(For JLab ULO use only.)

List below significant resources — both equipment and human — that you are requesting from Jefferson Lab in support of mounting and executing the proposed experiment. Do not include items that will be routinely supplied to all running experiments such as the base equipment for the hall and technical support for routine operation, installation, and maintenance.

Major Installations *(either your equip. or new equip. requested from JLab)*

None

New Support Structures: None

Data Acquisition/Reduction

Computing Resources: CODA

New Software: none

Major Equipment

Magnets: None additional

Power Supplies: None additional

Targets: LH2 unpolarized

Detectors: HMS + SOS

Electronics: Standard

Computer Hardware: Standard

Other: None

Other:

Spin Polarization in Kaon Electroproduction

Jefferson Lab Proposal

Abstract

This proposal describes an experiment to study spin polarization observables in kaon electroproduction. The experiment will use a longitudinally polarized electron beam, an unpolarized hydrogen target, and will be sensitive to the Λ-hyperon recoil polarization. In the electromagnetic production of kaons from a proton, $e + p \rightarrow e' + K + \Lambda$, the associated Λ-hyperon will be identified by its missing mass in the reaction, and the decay proton from the hyperon ($\Lambda \rightarrow p + \pi$) will be detected. Because the Λ-hyperon is self-analyzing, a measurement of the proton momentum distribution may be used to determine the hyperon spin polarization vector. Thus the experiment will serve to elucidate the process of polarization transfer from the polarized electron to the Λ-hyperon as well as induced hyperon polarization which results even for an unpolarized beam. (Induced polarization has been studied previously using real photons. However, this will be the first measurement at nonzero momentum transfer.)

The cross section $\sigma_{TT'}$ and $\sigma_{TL'}$ will be measured for squared four-momentum-transfer, Q^2, from 0.5 to 2.1 $(GeV/c)^2$. Additionally, because the hyperon recoil polarization will be measured simultaneously, the polarization transfer response functions, $R_{TT'}^{z'0}$ and $R_{TL'}^{x'0}$ will be determined in this same kinematic range. Kaons (hyperons) will be detected along (opposite to) the momentum-transfer direction in the center-of-mass frame. In the laboratory frame, both kaon and hyperon momentum vectors lie parallel to the momentum transfer direction. The experiment will be carried out with standard equipment in Hall C, viz., the cryogenic unpolarized (liquid) hydrogen target, and the HMS and the SOS with the same detector packages that were used in the kaon electroproduction experiments completed in the fall of 1996.

Spin observables may be used to shed light on the hyperon spin structure and the spin dependence of the partonic fragmentation and recombination processes. Additionally, the response functions $R_{TT'}^{z'0}$ and $R_{TL'}^{x'0}$ exhibit some sensitivity to the Λ-hyperon electromagnetic form factor at nonzero Q^2 ($Q^2 > 0$). Presently, this is the best way to measure hyperon form factors for large space-like momentum transfer.

Overview

Strangeness electroproduction, that is, the electromagnetic production of hadronic systems with constituent strangeness, remains one of the forefront areas of research in nuclear and particle physics at intermediate energies. The CEBAF accelerator at Jefferson Lab has proven to be a powerful tool for use in studying the electromagnetic production of hadronic systems containing a strange constituent quark. The electromagnetic probe only marginally disturbs the system being investigated, and is well understood [1-6]. Its use as a means to probe the internal structure of hadronic systems has been well documented. Among the most studied of these hadronic systems is the nucleon. The unique opportunities afforded by the use of polarized, high-current, high-duty-factor electron beams provides an even more powerful probe of the electromagnetic structure of hadronic systems; the study of the spin dependence of the electromagnetic production and weak decay of the hyperon, specifically the Λ-hyperon, becomes feasible. This proposal describes an experiment to study the electroproduction of the Λ as a function of virtual photon momentum transfer, angle, and energy, using spin polarization observables in order to extract insights into its production and weak decay dynamics.

The free Λ-hyperon has a lifetime, τ_Λ, of about 3×10^{-10} s; it exhibits two main decay modes, both mesonic:

$$\Lambda \rightarrow p + \pi^- + 37.8\ MeV \quad (0.642) \qquad \text{(EQ 1)}$$

$$\Lambda \rightarrow n + \pi^0 + 41.1\ MeV \quad (0.358) \qquad \text{(EQ 2)}$$

Here the number in parenthesis shows the decay branching fraction. Consider the free decay of a Λ-hyperon into a proton and pion. (Similar arguments apply to the decay into a neutron and neutral pion.) The proton and pion are emitted back-to-back in the Λ rest frame. Normally, it is not necessary to detect the pion in a Λ decay experiment in order to determine the decay mechanism because of these constraints (momentum conservation as well as the self-analyzing nature of the decaying hyperon). The decay given in (1) is easier to detect, generally, since it has the larger branching fraction and since the proton is easier to identify than the neutron. The production and decay of the Λ-hyperon can be studied in ways not feasible before now, as presented in this proposal.

The current experiment aims to study the production of Λ-hyperons using a

polarized beam as well as study the mechanism of polarization transfer in the reaction

$$\vec{e} + p \rightarrow e' + K + \vec{\Lambda} \qquad \text{(EQ 3)}$$

A polarized electron beam and the existing unpolarized cryogenic hydrogen target in Hall C are required for this measurement. The hyperon induced polarization (which results even with an unpolarized beam) will be measured simultaneously. The experiment will use the HMS and the SOS in Hall C to detect, respectively, the scattered electron and the electroproduced kaon before it decays in flight. Additionally, the SOS will be used to detect the proton from the hyperon decay. The SOS used as a hyperon tagger, in general terms, will detect the protons resulting from the weak decays of the hyperons in

$$\vec{\Lambda} \rightarrow p + \pi \qquad \text{(EQ 4)}$$

The hyperon is self-analyzing; its polarization will be determined by measuring the angular distribution and the momenta of the protons (from the hyperon decays) with respect to the hyperons' spin and momenta directions. Both the kaon and the hyperon-decay proton in this measurement will be detected along the virtual photon direction (in the laboratory frame). Thus the SOS will serve the dual purpose of identifying the kaon electroproduction reaction as well as tagging the hyperon spin polarization vector. This is explained more carefully in the section on the experimental setup and procedure in this proposal.

Once the momenta of the scattered electron and electroproduced kaon from (3) are measured, the hyperon momentum and energy are determined. Then, since the decay (1) is well known, only the proton needs to be detected in order to determine the hyperon spin in the proposed measurement; the pion does not need to be detected. The hyperon momentum will be high enough so that the protons from the decay will lie in a rather tight cone centered on the hyperon momentum vector; the decay proton will be detected by the hyperon tagger (the SOS) for all hyperon spin directions. At the same time, the hyperon momentum will be low enough so that reasonable angular resolution can be achieved for proton detection in the reaction (4). Time-of-flight information in the SOS will be used to identify the kaon and the proton and to determine their momenta.

To lowest order in the fine structure constant $\alpha = \frac{e^2}{4\pi} \approx \frac{1}{137}$, the electron interacts

with the hadronic current through the exchange of a single virtual photon with well defined energy transfer $\nu = E_i - E_f$ and momentum transfer $\vec{q} = \vec{k}_f - \vec{k}_i$. The kinematics of the electron scattering process is determined by three independent kinematical variables, usually chosen to be the invariant energy of the system, W, the scattering angle in the center of mass system θ, and the squared four-momentum-transfer $Q^2=-q^2$. The nucleon four-vectors are $P_N=(E_N,\mathbf{P_N})$ for the initial and final states. It can be shown that the most general expression for a coincidence experiment considering an experiment with three types of polarization, target, beam, and recoil, is

$$\frac{d^5\sigma}{d\Omega_f d\Omega_K d\varepsilon_f} = \Gamma \frac{d\sigma_v}{d\Omega_K} \qquad \text{(EQ 5)}$$

$$\frac{d\sigma}{d\Omega_K} = \frac{|k|}{k_\gamma^{cm}} P_\alpha P_\beta \Big\{ R_T^{\beta\alpha} + \varepsilon_L R_L^{\beta\alpha} + \sqrt{2\varepsilon_L(1+\varepsilon)} R_{TL}^{\beta\alpha} \cos\phi_K + \sqrt{2\varepsilon_L(1+\varepsilon)} R_{TL}^{\beta\alpha} \sin\phi_K + \varepsilon(R_{TT}^{\beta\alpha}\cos 2\phi_K + R_{TT}^{\beta\alpha}\sin 2\phi_K) + h\sqrt{(1-\varepsilon_L)2\varepsilon_L}({}^{c}R_{TL'}^{\beta\alpha}\cos\phi_K + {}^{s}R_{TL'}^{\beta\alpha}\sin\phi_K) + h\sqrt{1-\varepsilon^2} R_{TT'}^{\beta\alpha} \Big\} \qquad \text{(EQ 6)}$$

using the notation of reference [7] and Fig. (1). Here k_γ^{cm} denotes the virtual photon center-of-mass momentum, the R's are the response functions with the superscripts α and β denoting the target and recoil polarization quantities, respectively, and the superscripts c and s denoting the term proportional to $\cos\phi$ and $\sin\phi$ respectively, ϕ_K is the azimuthal angle between the electron scattering plane and the reaction plane, Γ is the virtual photon flux, and (ε_L) ε is the (longitudinal component of the) virtual photon polarization parameter. The response functions are bilinear combinations of the elementary amplitudes for kaon electroproduction. The expressions for these functions written in terms of the elementary amplitudes can be found in [2,7]. Note that in the notation of reference [7], the polarization is written P = (1,**P**), so that the P_0 component

remains even when there is no target (or recoil) polarization. $P^{\alpha} = (1,\mathbf{P})$ and $P^{\beta} = (1,\mathbf{P'})$ where $\mathbf{P} = (P_x, P_y, P_z)$ and $\mathbf{P'} = (P_{x'}, P_{y'}, P_{z'})$ denote the target and recoil hyperon polarization vectors, respectively.

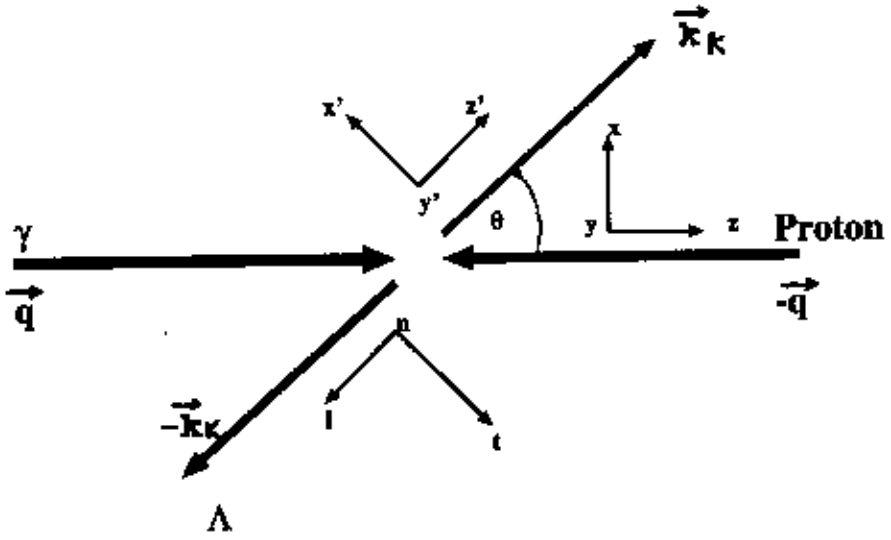

Figure (1). The kinematics of the polarization transfer reaction. Polarization gets transferred from the electron to the Λ-hyperon with the emergent hyperon and kaon momenta lying along the momentum transfer direction. The three spin axes of the hyperon in its rest frame are shown.

In the specific case of polarized electron scattering (flipping the electron spin vector), no target polarization, and determination of the polarization of the decaying hyperon when the hyperon is detected at small polar angles $\theta_{K\gamma}$ along the q-vector, the equation reduces approximately to

$$\frac{d\sigma_v^{for}}{d\Omega_K} - \frac{d\sigma_v^{bak}}{d\Omega_K} =$$

$$2\left(P_\beta \frac{|k|}{k_\gamma^{cm}} \sqrt{2\varepsilon_L(1-\varepsilon_L)}({}^{c}R_{TL'}^{x'0}\cos\phi_K)\right) +$$

$$2\left(P_\beta \frac{|k|}{k_\gamma^{cm}} \sqrt{1-\varepsilon^2}\, R_{TT'}^{z'0}\right) \qquad \text{(EQ 7)}$$

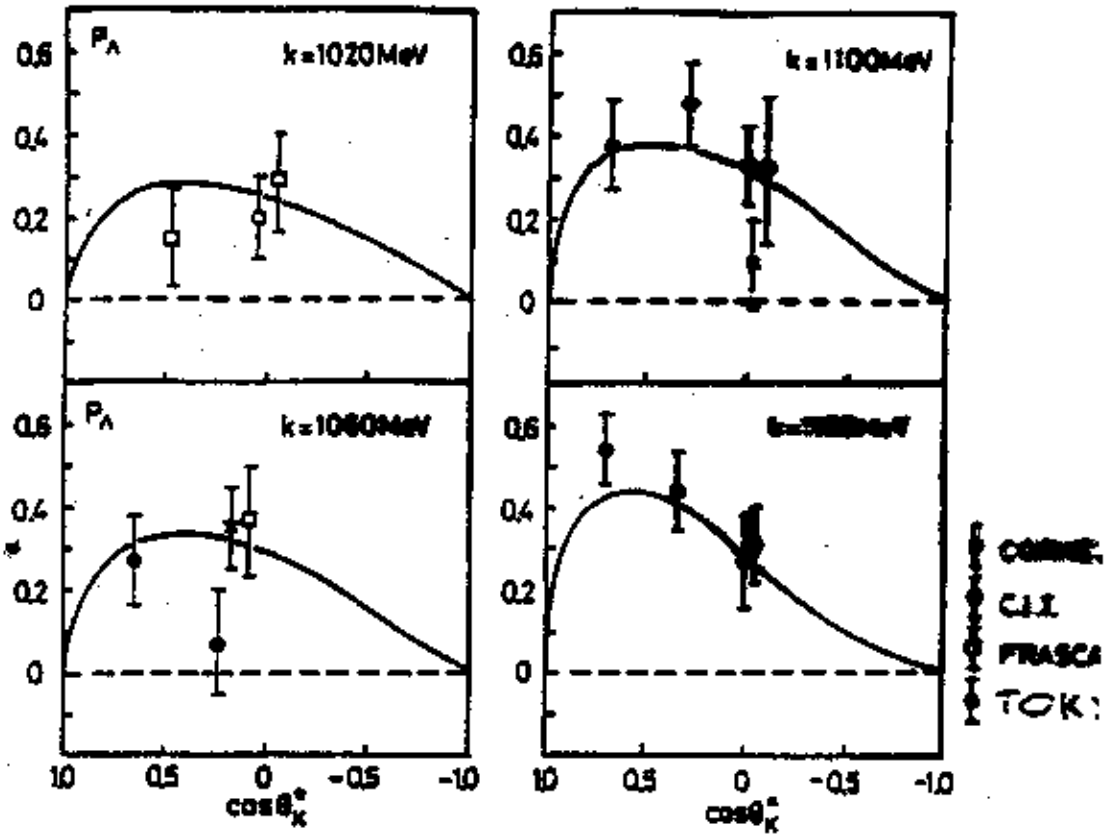

Figure (2). The <u>induced</u> polarization in the kaon <u>photoproduction</u> reaction (3), from reference [9]. The experiment described in this proposal will study polarization <u>transfer</u> and high-Q^2 <u>induced</u> polarization at small center of mass angles.

The measurements of the helicity dependent cross sections $\sigma_{TT'}$ and $\sigma_{TL'}$ will serve to constrain kaon electroproduction models, similar to the way the

unpolarized cross section data from Experiment E93-018 was used to gain further insights into the strangeness production mechanism. These cross sections will be measured in the range Q^2= 0.45 to 2.06 $(GeV/c)^2$. The measurement of the complete set of cross sections in kaon electroproduction with associated Λ production at forward angles will be achieved in this experiment. The first two terms of equation (6) have been measured recently in Jefferson Lab Experiment E93-018. The interference terms have been measured previously (there is some sensitivity to these terms from E93-018 as well). The two terms proportional to the electron helicity have not been measured previously and will be studied in this experiment. The hyperon polarization (both helicity dependent and helicity-independent) will be determined in the measurement, so that the helicity dependent response functions $R_{TT'}^{z'0}$ and $R_{TL'}^{x'0}$ will be determined in this same kinematic range.

The helicity-independent (induced) hyperon polarization remains even when the incident electron beam is unpolarized [8-9]. The induced polarization will be nonzero for a subset of the measurements (for $\theta_{K\gamma} \neq 0^o$ or 180^o) and will vanish in the subset of data where desired (see Fig. (2)). The hyperon induced polarization vector lies in a plane which is orthogonal to the reaction plane (containing the hyperon momentum vector and the kaon momentum vector). The polarization transfer (helicity-dependent) vector lies in the reaction plane and will be orthogonal to the induced polarization vector. Both polarizations will be measured independently in the experiment.

From these polarization measurements, several physics issues can be studied in ways not feasible or even possible previously. Two examples are given in the following section; the dynamics of spin polarization at nonzero Q^2 in hyperon production and the Λ-hyperon form factor at high Q^2. This will be done by measuring the three hyperon spin components along x', y', and z' (or equivalently **l**, **t**, and **n**).

Physics Motivation

Hyperon Spin Dynamics

It has been known for some time that Λ-hyperons can acquire a sizeable (induced) polarization even when produced using an unpolarized beam and target. This phenomenon is observed in both hadron-induced and well as electromagnetic-induced hyperon production. There are several possible explanations of this effect. Most require the interference between low-lying baryon and meson resonances in the production process giving rise to rather large spin polarization. The polarization would be expected to vanish at high energies since, among other things, the contribution of several production channels with large multiplicities of final states make it unlikely to have coherent interference between spin nonflip and spin flip amplitudes which would lead to sizeable induced polarization. The observation of rather large induced polarization seen in hyperon production at high energies suggest a more complex picture of the process. More studies at high energies are needed to disentangle the physics. While there is recent data for polarization transfer in hadron-production of hyperons [10] and proposals to study induced polarization in photoproduction at Jefferson Lab [9], by contrast there is no data for polarization transfer from a polarized electron beam to a polarized hyperon in the electroproduction process. Nor is there data for induced polarization with virtual photons.

The polarization transfer mechanism should give further insights into the role (if any) strange quarks play in hyperon structure; for example, no correlation is expected between incident electron polarization and the hyperon spin polarization in associated production of kaons and hyperons, because the Λ spin is thought to be carried entirely by its constituent *strange* quark, while the *ud* di-quark (in a spin and isospin singlet state) propagates unperturbed as a spectator in the interaction [10]; there is no constituent strangeness in the initial system (electron and target proton. In that case, spin asymmetries related to the beam polarization are expected to vanish. If the polarization transfer from the electron to the hyperon is large, then this may signify that the *ud* di-quarks play a more prominent role in the recombination process than expected. The results of this study should shed light on this phenomena.

Additionally, it has been shown that the electroproduction of fast hyperons along the direction of the virtual photon can serve to illuminate the aptitude of the quarks to carry transverse polarization in the hyperon system [11]. The Λ is a uds isosinglet quark system. In the nonrelativistic quark model, if the up and down

quark pair form a spin-zero core, the strange quark can carry most of the observed fraction of the spin of the hyperon. A measurement of the hyperon recoil polarization and the response functions $R_{TL'}$ and $R_{TT'}$ over a broad range of Q^2 will yield information on these dynamics.

Hyperon Electromagnetic Structure

There has been much recent interest in the study of the internal structure of baryons. Form factors are employed to describe the internal structure of hadronic systems [12-17]. Concurrently, nucleon form factors provide much needed, fundamental input for nucleon and nuclear structure models. The electric and magnetic form factors of neutrons and protons continue to be among the highest priority subjects in this field.

The marriage of these two subjects - strangeness electroproduction and nucleon form factors - results in a tantalizing new area for investigation, that of hyperon form factor measurements. The present proposal describes an experiment which is potentially sensitive to the electric and magnetic form factor of the Λ-hyperon at moderate momentum transfers. This information is fundamentally important in both nuclear and particle physics. The electroproduction of kaons with the associated production of hyperons (using polarization observables) is the most powerful means of extracting this information at large Q^2.

Presently, the only recoil polarization data in kaon electroproduction comes from the study of induced hyperon polarization [8-9,18] as shown in Fig. (2). (The kaon, being pseudoscalar, carries no spin polarization.) This experiment is the first proposed to study polarization transfer in the manner described in this proposal.

The earliest studies of the electromagnetic structure of the nucleons using moderate energy electromagnetic probes can be traced back to the work of Hofstadter and collaborators at Stanford [19]. It was shown that the electromagnetic probe interacts with the internal charge and current distribution of the nucleon - that is to say that the nucleons are not point objects, microscopically. The electromagnetic form factors are a measure of the deviation of these systems from pure point-like objects. The full momentum transfer dependence of these form factors cannot be calculated from first principles (quark and gluon degrees of freedom) over a large momentum transfer range. Experimental measurements combined with model calculations remain the only way to determine these quantities presently. Reasonable understanding of the

internal structure of the baryons is necessary for progress in the field of intermediate-energy nuclear and particle physics [20].

The most accurate experimental data that exists for nonzero momentum transfers is for the electric and magnetic form factors of the proton. Less precise data exist for the neutron. While these quantities have been measured reasonably well over a large momentum transfer region, there exists no data for the corresponding systems which contain a strange constituent quark, that is to say, hyperons. The polarization transfer response functions exhibit some sensitivity to $G_E^{\Lambda}(Q^2)$ and $G_M^{\Lambda}(Q^2)$, the Λ electric and magnetic form factors at nonzero momentum transfer.

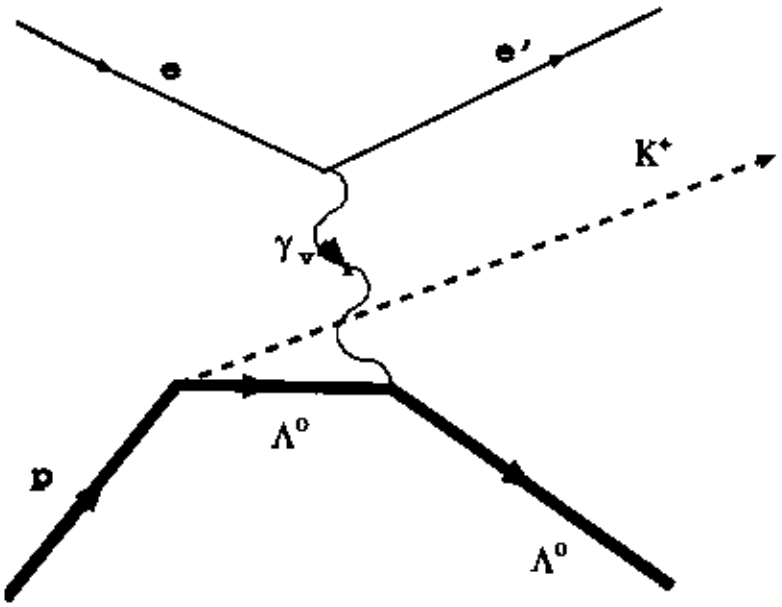

Figure (3). The Feynman diagram for the process of interest for the hyperon form factor. The virtual photon couples directly to the hyperon.

The process to be studied is given by expression (3) and (4). The Feynman diagram of interest describing the process is shown in Fig. (3). The virtual photon from the electron scattering vertex couples directly to the Λ-hyperon. Unfortunately, there are several other processes which contribute to the physics quantity measured.

For most of the background processes which contribute, the polarization transfer mechanism provides a clean way for identification. These processes 'decay' into a kaon and hyperon. The maximum hyperon polarization in these processes

combined is expected to be no more than 1/3 of the polarization transfer measured in the process of Fig. (3) [11,21-22]. The most insidious of the background processes is the coupling of the virtual photon to a Σ-hyperon which then decays into Λ-hyperon. Experimental data confirms the theoretical prediction that the coupling the Σ-hyperon, $g_{KN\Sigma}$, is much weaker than the coupling to the Λ-hyperon, $g_{KN\Lambda}$. This background contribution is therefore expected to be small.

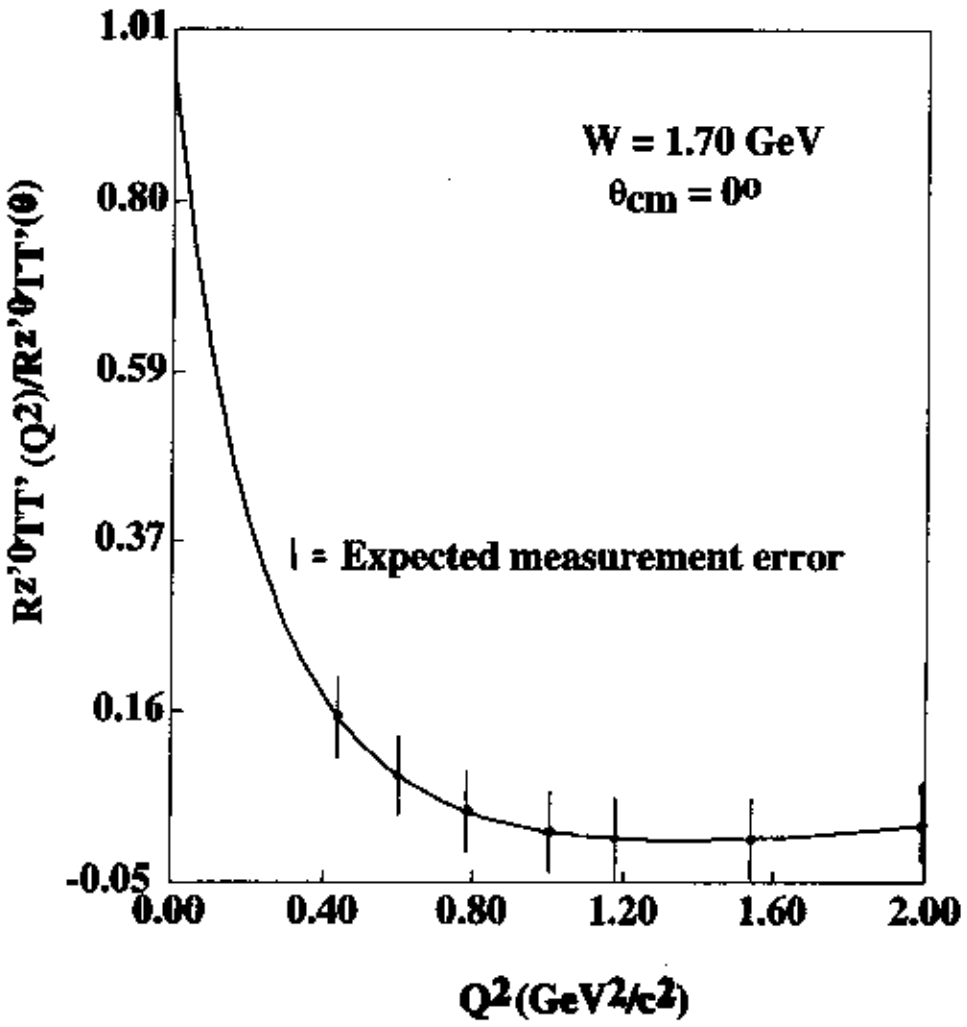

Figure (4). The Q^2 dependence of the polarization transfer coefficient which will be measured in this experiment. The calculation is by R. Williams [23]. The expected measurement error of the data is shown.

The Q2 dependence of the polarization transfer response function $R_{TT'}^{z'0}$ is shown in Fig. (4). The curve is a calculation using the results of Williams [23] for invariant energy (W) of 1.70 GeV, the same as will be used experimentally. The calculation includes on Born diagram terms with s and u channel resonances and excludes, for example, K* exchange in the t-channel process. This is justified on the basis of duality arguments [23]. Also plotted on the curve is the expected precision of the measurement at the seven experimental points. It is reasonable to expect a 10-12% measurement precision as shown in the next section of this proposal. The sensitivity of the measurement to the hyperon form factors is shown in Fig. 5.

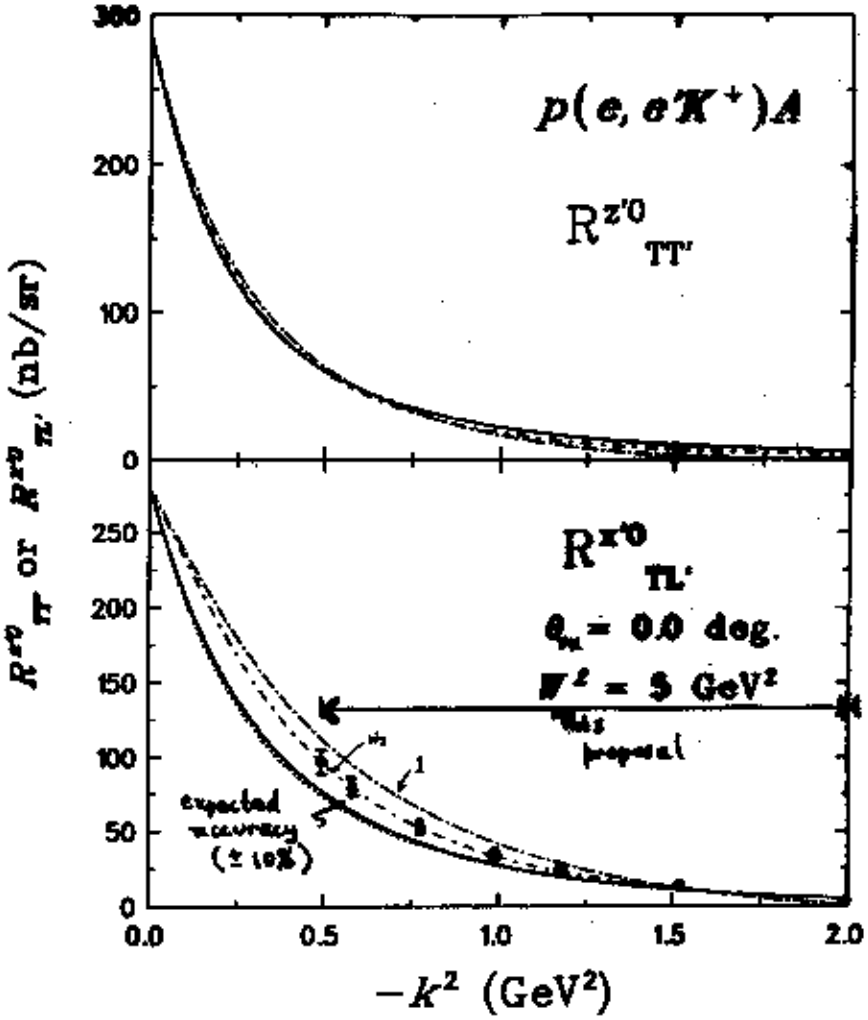

Figure (5). The polarization transfer response function sensitivity to the hyperon form factor versus squared momentum transfer. Four different values of the form factor are input which yield the curves for $R_{TT'}$ in the top figure and $R_{TL'}$ in the bottom figure. Calculation by C. Bennhold and T. Mart [24].

Experimental Setup and Procedure

The experimental setup uses the HMS and the SOS in Hall C, with the SOS employed as a hyperon tagger, in addition to its role as a kaon detector. A polarized electron beam of up to 30 μA current with a nominal 80% polarization (or whatever is the maximum electron polarization when the experiment is run) will impinge upon the unpolarized cryogenic hydrogen target.

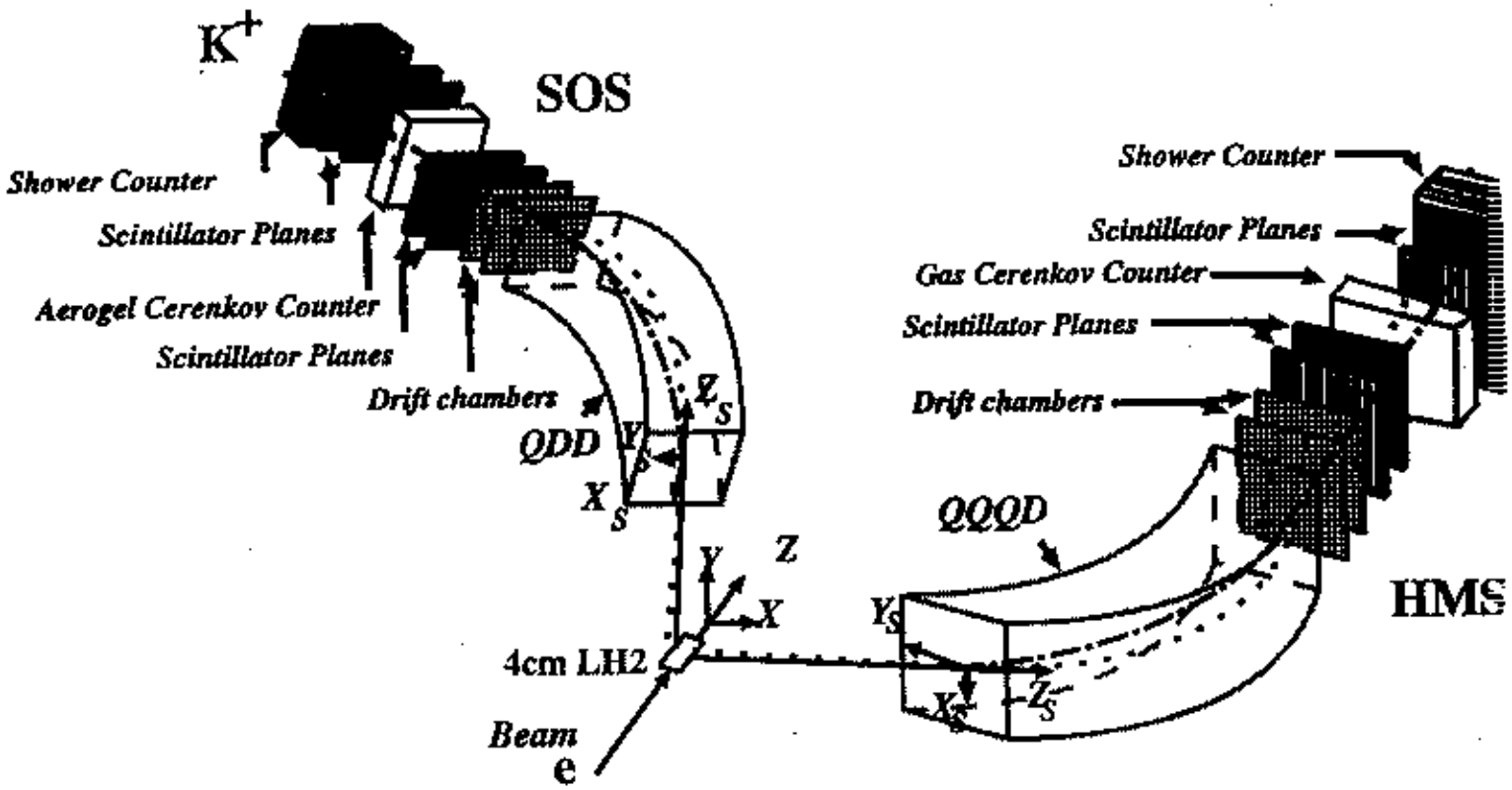

Figure (6). The experimental setup in Hall C. The HMS and SOS will be used to detect, respectively, the scattered electron and electroproduced hyperon, while, additionally, the SOS will detect the proton from the hyperon weak decay.

The HMS will be used to detect the scattered electron, while the SOS will be used to identify the electroproduced kaon before its decay in flight, as well as detecting

the proton from the hyperon decay. The hyperon tagger (SOS) will be used to determine the hyperon momentum and spin by measuring, respectively, the kaon momentum and the momentum of the nucleon from the decay given in (4).

The Hall C setup is shown schematically in Fig. (6). This is the same setup that was used in the previous kaon electroproduction experiments (E91-016 and E93-018) which were completed in the fall of 1996. In those series of measurements, the angles and momenta of the coincident electrons and kaons were reconstructed.

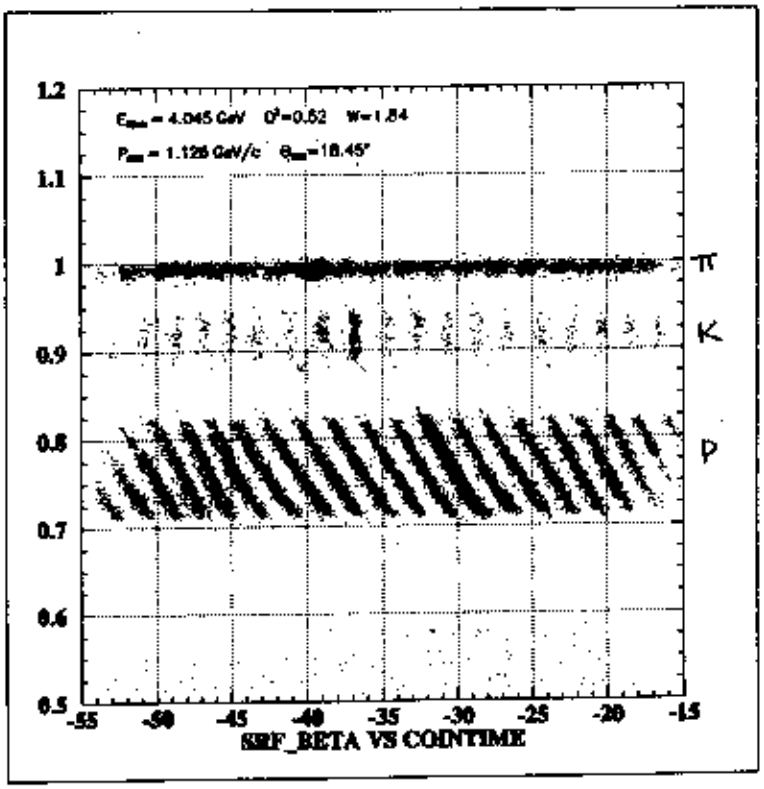

Figure (7). The particle velocity versus the coincidence time for the particles detected in the SOS during Experiment E93018. The horizontal bands correspond to pions, kaons, and protons detected in coincidence with the scattered electrons.

A plot of the velocity (with respect to the speed of light), β, of the particles detected in the SOS versus the coincidence time is shown in Fig. (7) for one of the kinematic settings. The particles at $\beta = 1$ are the pions, the slower particles at $\beta = 0.8$ are the protons, while the particles between these two extremes in β are the kaons. Projection along the coincidence time axes after application of particle identification cuts (to separate the pions and protons) shows a clear kaon peak (in-time, real coincident kaons) and indicates very little random coincident background, relative to real coincidences (see Fig. (8)).

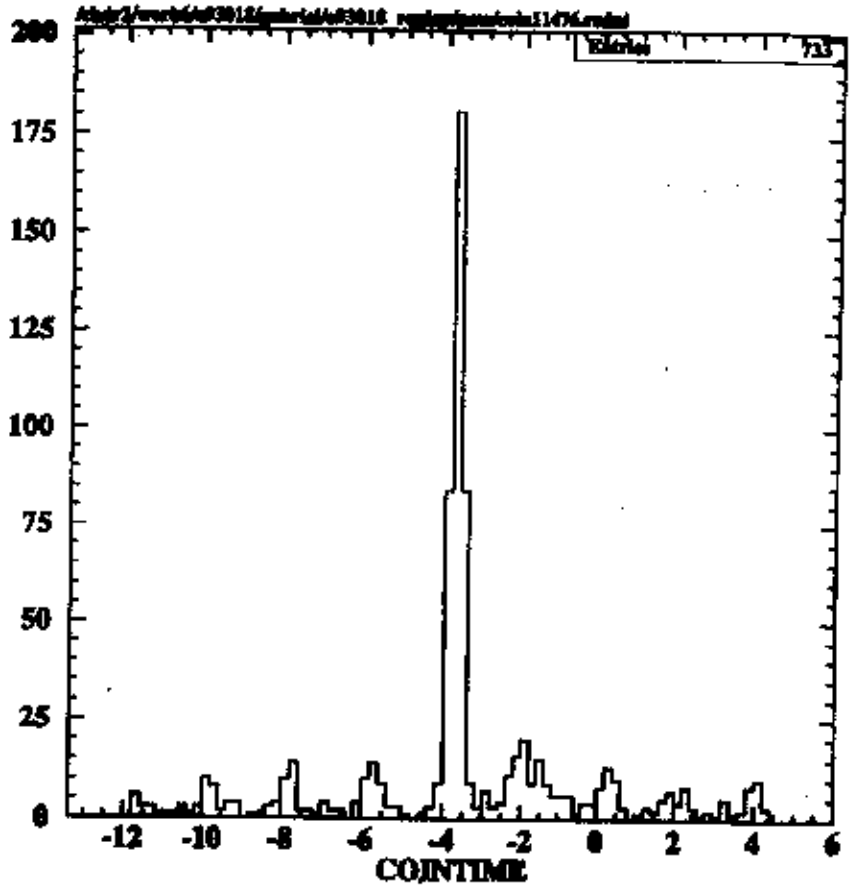

Figure (8). Projection of the events from the previous figure along the coincidence time axis shows the in-time as well as random coincident kaons. This data from E93018 is used to compute the missing mass spectrum.

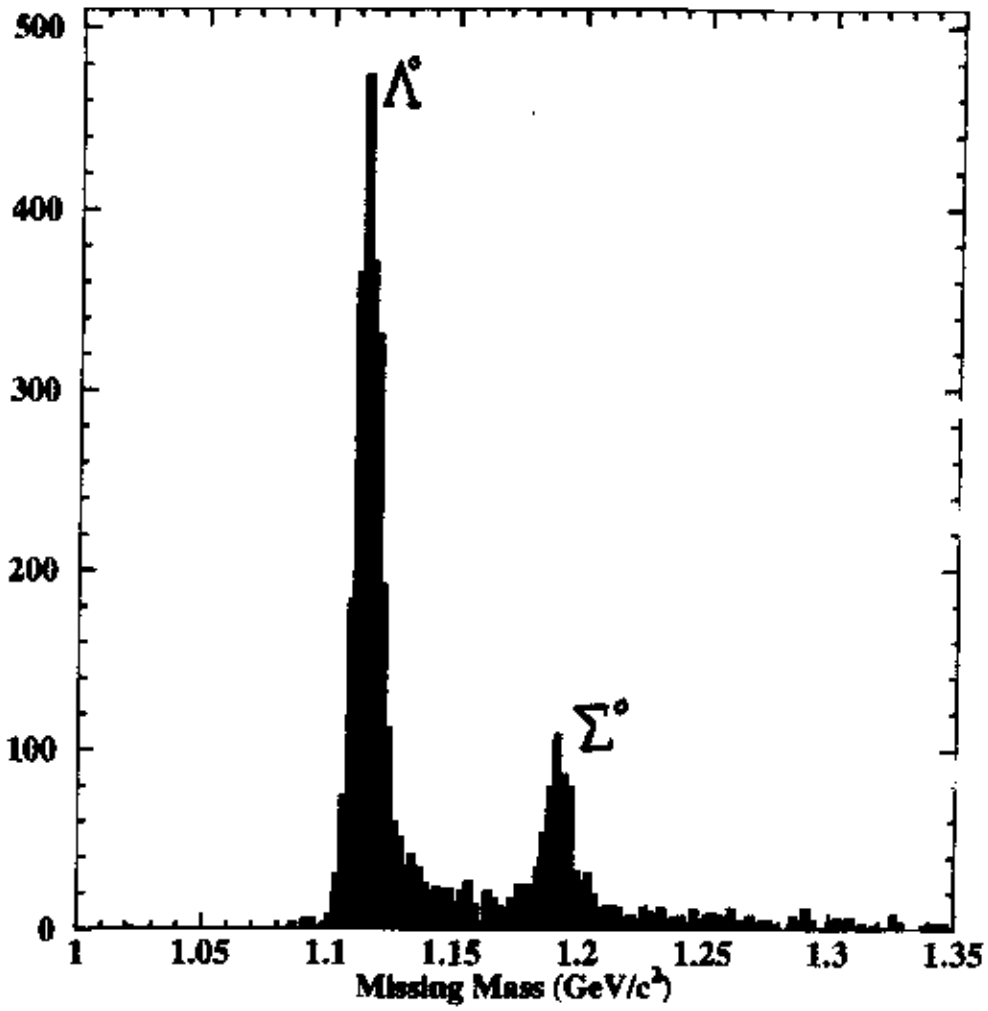

Figure (9). The calculated missing mass spectrum based upon the electron - kaon coincidences from E93018. The Λ and Σ-hyperons are clearly identified.

Once the scattered electron and the electroproduced kaon are detected (in coincidence), the reaction in (3), but with no polarization observed in the initial or final state, is then kinematically complete; the calculated missing mass spectrum indicates clearly separated Λ and neutral Σ-hyperons, as seen in Fig. (9).

The experiment described in the present proposal will use the same techniques to identify the Λ-hyperons in the reaction of equation (3). The Λ spin direction and momentum are fixed once the kaon and electron in the coincidence event are detected. The SOS will then be placed in the appropriate position (angle and momentum settings) to detect the nucleon from the decay reaction in equation (4).

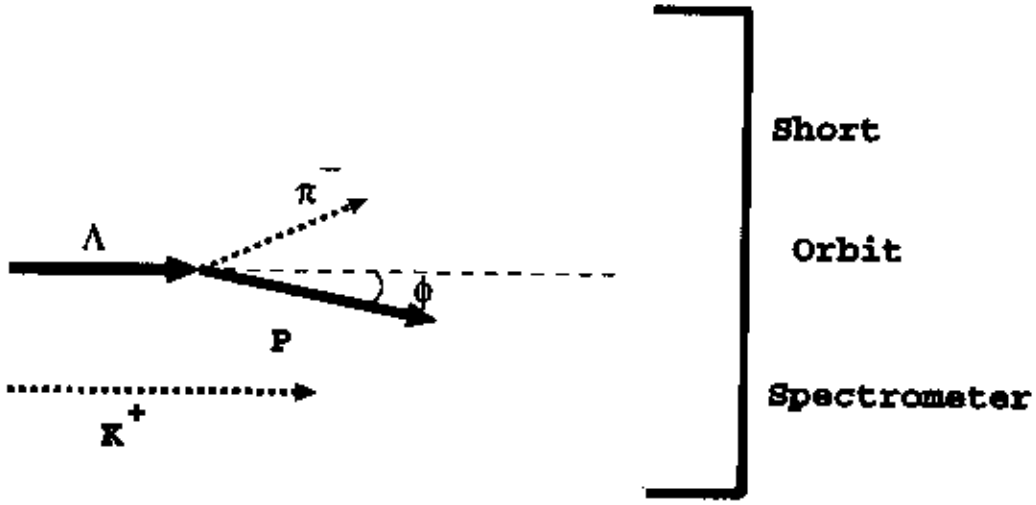

Figure (10). The SOS used as a hyperon tagger. The decay protons from the reaction (4) are detected in the SOS spectrometer, thus tagging the hyperon spin polarization vector.

In the rest frame of the Λ–hyperon, the proton and pion emerge back - to - back. In the laboratory frame, both the nucleon and the pion from the decay are detected in the forward direction (at these hadron momenta) as shown in Fig. (10). The decay proton will lie in a rather narrow angular cone about the direction of the electroproduced hyperon. The size of this cone, and therefore the dimensions of the hyperon tagger, is dictated by the Λ momentum. The hyperon spin polarization about each of the three spin axes considered is determined by the angular distribution of the protons using the expression (valid in the hyperon rest frame)

$$\frac{dN}{d\Omega_p} \propto (1 + \alpha P_\Lambda(\hat{s} \cdot k_p)) = (1 + \alpha P_\Lambda \cos\theta_{ps_\Lambda}) \qquad \text{(EQ 8)}$$

where k_p is the proton momentum, θ_{ps_Λ} is the angle between the hyperon spin vector and the proton momentum vector, α is the weak decay correlation coefficient (experimentally determined to be 0.642 ± 0.013 [21-22]), and P_Λ is the magnitude of the hyperon spin polarization in the given direction being considered (see Fig. (1)). The angle θ_{ps_Λ} will be measured with an accuracy of better than 3 mr while the relevant momenta will be determined with an accuracy of 10^{-3}. Both angular and momentum accuracy are needed to precisely determine the hyperon decay proton angular distribution in (8). This level of precision was achieved in the previous Hall C kaon electroproduction experiments (E91-016 and E93-018).

TABLE 1. Kinematics

Q^2	E_{in}	E_{out}	θ_e	θ_γ	ν	W
0.455	4.045	2.800	11.500	23.200	1.245	1.662
0.604	4.045	2.700	13.500	23.941	1.345	1.674
0.765	4.045	2.600	15.500	24.290	1.445	1.681
0.990	4.045	2.500	18.000	24.860	1.545	1.670
1.171	4.045	2.400	20.000	24.638	1.645	1.672
1.539	4.045	2.200	24.000	23.734	1.845	1.674
2.059	4.045	1.900	30.000	21.599	2.145	1.687

The kinematic parameters for the present experiment are listed in the tables above and below. The incident electron energy is fixed at 4.045 GeV. At each Q^2 point, the hadron spectrometer (the SOS) will be fixed in angle along the virtual photon direction (parallel kinematics) for the extraction of $R_{TT}^{z'0}$ and $R_{TL'}^{x'0}$ (where the induced polarization is zero), and for small nonzero angles (within the SOS angular acceptance) with respect to the virtual photon when nonzero induced polarization is desired. In each Q^2 setting, the hyperon and kaon laboratory momenta are well matched for the simultaneous detection of kaon and decay protons.

TABLE 2. Kinematics (continued)

Q^2	ε	p_γ	p_{sos} ($=p_K$)	p_Λ ($=p_p$)	$\theta_{\gamma\Lambda}$	time (days)
0.455	0.918	1.416	0.704	0.712	0.00	1.5
0.604	0.899	1.553	0.790	0.763	0.00	1.5
0.765	0.879	1.689	0.866	0.823	0.00	1.5
0.990	0.854	1.838	0.898	0.940	0.00	2.0
1.171	0.829	1.969	0.960	1.011	0.00	2.0
1.539	0.775	2.223	1.072	1.151	0.00	2.0
2.059	0.683	2.581	1.267	1.314	0.00	2.5

It should be emphasized that this particular measurement has never been attempted before in this manner, and it is most feasible at CEBAF because of the control of the Λ momentum and spin direction. In the case of the $R_{TT'}$ and $R_{TL'}$ measurement, a statistical accuracy at each data point of approximately 3% is predicted, on average.

The HMS detector and background estimates

The choice of electron momentum and angle for the experiment is dictated by several considerations:

1. *The electroproduction cross section is a moderately strong function of the virtual photon momentum in this region. Large kaon (and therefore Λ) count rates are needed.*
2. *Sufficient photon momenta are necessary so that the emergent kaons have enough momenta that a large fraction are detected before decay in the SOS.*
3. *The minimum HMS angle. Small angles are favored, in some cases.*

The HMS will be used in the point-to-point tune mode (the same as was used in E93-018). The largest contribution to the reconstructed electron momentum accuracy in the HMS resolution is $\Delta p/p < 10^{-3}$. The detector stack for the HMS detector is shown in Fig. (6). The detector stack uses standard focal plane instrumentation and is the same configuration used in E93-018. There will be drift chambers for charged particle tracking, a gas Cherenkov detector for particle identification, scintillator hodoscopes for fast timing, and Pb-glass shower counters for calorimetry.

Charged particle trajectories will be measured using 2 multiwire drift chambers each having XYUVY'X' planes with the U and V stereo planes at 15° with respect to the X and X' planes. The X'(Y') planes are offset by one-half cell from the X(Y) planes. Thus there will be 12 multiwire planes before the scintillator hodoscopes or Cherenkov detector. Initial experiments which make use of the HMS drift chambers have shown that spatial resolutions of better than 170 μm (σ) can be expected up to the highest rates that will be encountered in the experiments using the HMS. This is sufficient to determine the angles and momenta to the desired levels experimentally.

The four planes of scintillator hodoscopes will be used for fast timing while the shower counters will be used for charged particle energy determination. The gas Cherenkov detector will be used mainly for π-e discrimination. Additionally, there should be some separation of charged particles from the Pb:glass shower counters. It has been demonstrated that pion-electron separations of 500/1 (achieved with this detector configuration) will be sufficient to reduce the backgrounds to acceptable levels.

The SOS Detector and Background Estimates

Kaon Kinematics

The choice of kaon momenta in the $p(\gamma_v,K^+)$ reaction is dictated by:

1. *The hyperon recoil momentum. A moderately large hyperon recoil momentum is needed so that the decay products are focussed in a rather small angular cone in the direction of the hyperon momentum.*
2. *The limits of the SOS spectrometer angles and momenta.*
3. *Matching the kaon and hyperon momenta.*

The SOS is a focusing spectrometer with a very short flight path (compared to the HMS). This short flight path enhances the detection of the short-lived kaons before their decay in flight.

The kaon (SOS) spectrometer will use standard focal plane instrumentation as shown in Fig. (6). There will be two sets of drift chambers (a total of 12 planes), measuring positions along X, Y, and U and V (stereo angles). Scintillator hodoscopes (four planes) will be used for fast timing, and an Aerogel Cherenkov counter for pion-kaon separation. It is advantageous, in the SOS, to use the time-of-flight differences between protons, pions, and kaons to identify these charged

particles (and therefore to separate them). By maximizing the distance between the S1 and S2 scintillator arrays in the SOS detector hut, charged particle separation has been easily achieved.

The proton-kaon time difference is large enough at all momenta that the time difference may be resolved. For the higher momentum settings, judicious use of the Aerogel Cherenkov counter and some time-of-flight separation may be used to yield a clean kaon signal. It has been demonstrated in previous Hall C experiments that using this system, a pion rejection (the most insidious problem) of approximately 1000 is achievable. This rejection ratio has been demonstrated in E93-018 to be adequate for this experiment [25].

The momentum of a charged particle will be determined by reconstructing its trajectory through the dipole (bending) magnet while the production angles are then obtained by tracing the trajectory through the quadrupole (focusing) magnets back to the target position. The maximum momentum acceptance is 20% (40%) while the solid angle is approximately 6.7 (7.7) msr for the HMS (SOS) spectrometer using the point to point tune. This technique will be used for both arms of the experiment.

The Hydrogen Target and Electron Beam

The (unpolarized) hydrogen target planned for the experiment will be 4.0 cm in length and 6.4 cm in diameter. This target container, cylindrical in shape, will have 0.08 mm thick aluminum end-windows. The effective length as 'seen' by each spectrometer is calculated based upon Monte Carlo simulation.

The uncertainty in the length of the target and target density is expected to be about 1 per cent. For the density, the calculated value based upon 19.0^{o} K temperature and 16 psi pressure (operating parameters) is 0.070 g/cm^3. For each point, a target empty and a target full run will be made in order to determine the background contribution coming from the target walls.

The experiment will use a longitudinally polarized electron beam with a maximum current of 30 μA and 80% polarization (or whatever is the maximum polarization available at the time of the experiment). The beam current will be measured using the standard beam current monitors in Hall C. The beam polarization will be measured using the Mott polarimeter which is currently being used in polarization measurements.

Electronics and Trigger

The experiment will use the CEBAF On Line Data Acquisition system (CODA) developed at CEBAF. The trigger in the HMS detector will consist of scintillator and Cherenkov detector signals to separate out electrons from pions and kaons (mainly) and antiprotons. Symbolically, the HMS trigger will be

$$S_1 \cdot S_2 \cdot C_e \qquad \text{(EQ 9)}$$

where S_1 (S_2) is the first (second) XY pair of scintillator hodoscopes, C_e is the gaseous Cherenkov detector which will fire on electrons and not pions or kaons. Time-of-flight separation will be adequate for e-K^- separation at all momentum in the experiment for the HMS. The SOS will use a trigger to separate out kaons from pions, positrons, and protons mainly. Symbolically, the hadron arm trigger will be

$$S_1 \cdot S_2 \cdot C_K \qquad \text{(EQ 10)}$$

where, again, S_1 (S_2) is the first (second) XY pair of scintillator hodoscopes and C_K is the aeorgel Cherenkov detector in the anticoincidence mode (the aerogel detector fires on pions and positrons in this momentum range). Time of flight separation is achievable at all momentum settings in this experiment.

The SOS as a Hyperon Tagger: Monte Carlo Simulation

A Monte Carlo simulation package has been developed which provides a good model of the Hall C setup to be used in this series of measurements. The software package was originally developed and used for a set of (e,e'p) experiments at SLAC [26] and later adapted to the Hall C configuration for use in the (e,e'K) experiments [27]. The Monte Carlo randomly generates the target quantities ($p_{e'}$, $\theta_{e'}$,$\phi_{e'}$) and (p_K, θ_K,ϕ_K) for the scattered electron and electroproduced kaon, respectively. The measured HMS and SOS angular and momentum acceptances are used. The energy and position (with simulated beam rastering) of the incident electron beam at the target were randomly generated and matched to the energy spread and spatial extent of the CEBAF beam (as observed in the recently completed kaon electroproduction experiments).

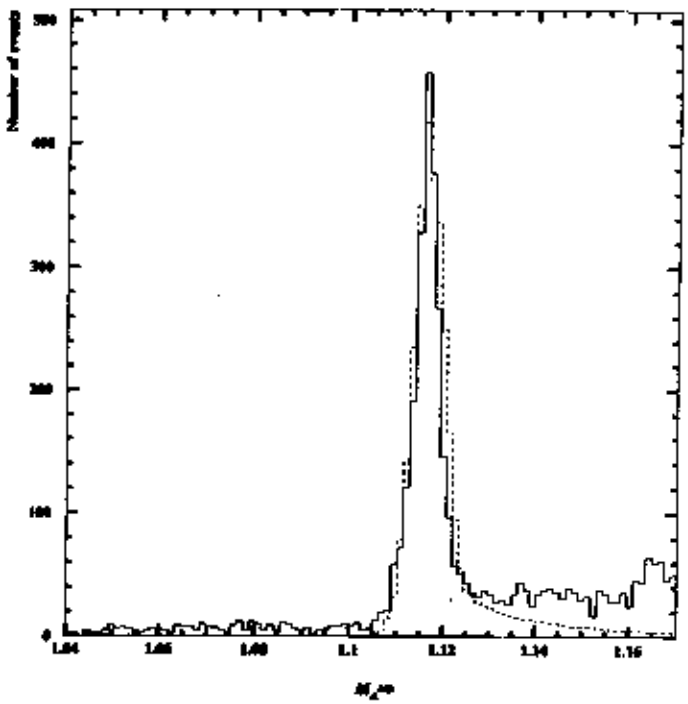

Figure (11). The missing mass spectrum generated from the reaction (3) where the kaon and electron are detected in coincidence in the SOS and HMS, respectively. The solid line is data from E93-018 and the dashed line is the Monte Carlo simulation.

From the position, the momentum, and the scattering angles of the charged particle at the entrance of each spectrometer, the code transports the particle through the (magnetic) optics to the detector hut in each case. COSY forward matrix elements for each of the different spectrometer elements are used to generate the relevant focal plane parameters. COSY backward matrix elements are then employed to determine the reconstructed target parameters. Conservation of energy and momentum are then used to generate the missing particle quantities (energy, momentum, and mass). The simulation includes energy loss and Coulomb scattering corrections to the particle trajectory through the material in the spectrometers from the target interaction point to the last detector element inside the detector hut. Fig. 11 shows the missing mass spectrum of reaction (3). The Λ-hyperon missing mass from the E93-018 data (solid line) compares well with the Monte Carlo simulation (dashed line).

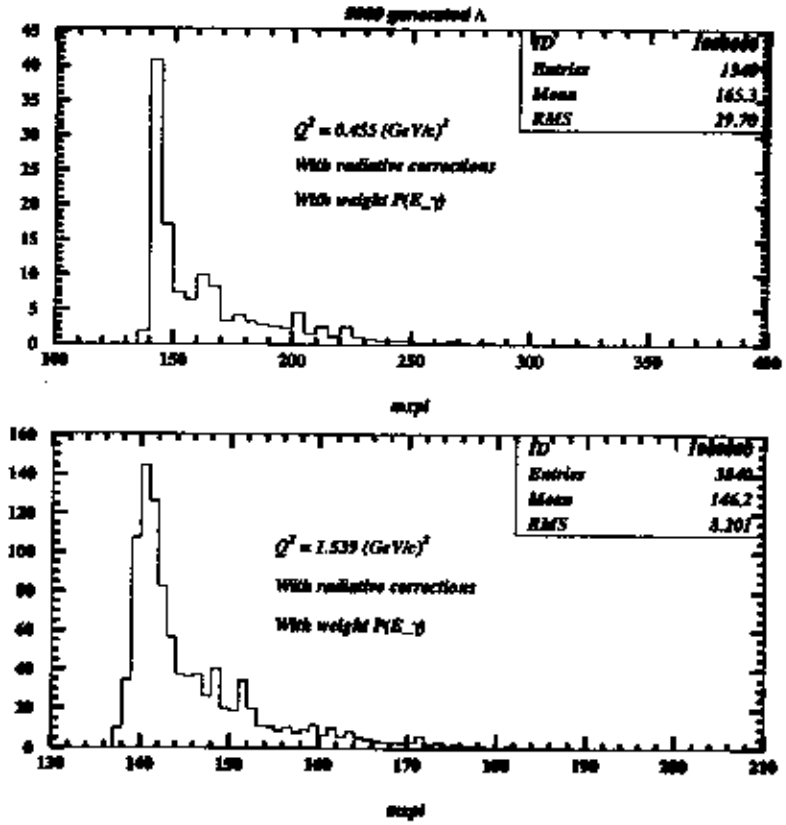

Figure (12). Simulation comparing the reconstructed pion missing mass from reaction (13) at two momentum settings, viz., 0.5 and 1.5 GeV^2/c^2.

Radiative corrections are applied to all charged particles which are detected; no radiative correction is applied to the Λ-decay pion since it is not detected. A

peaking approximation with hard and soft photon corrections is computed. Random photon energies from zero up to the proton kinetic energy are generated. The A-decay proton momentum and angles are modified accordingly before registering on the focal plane detectors.

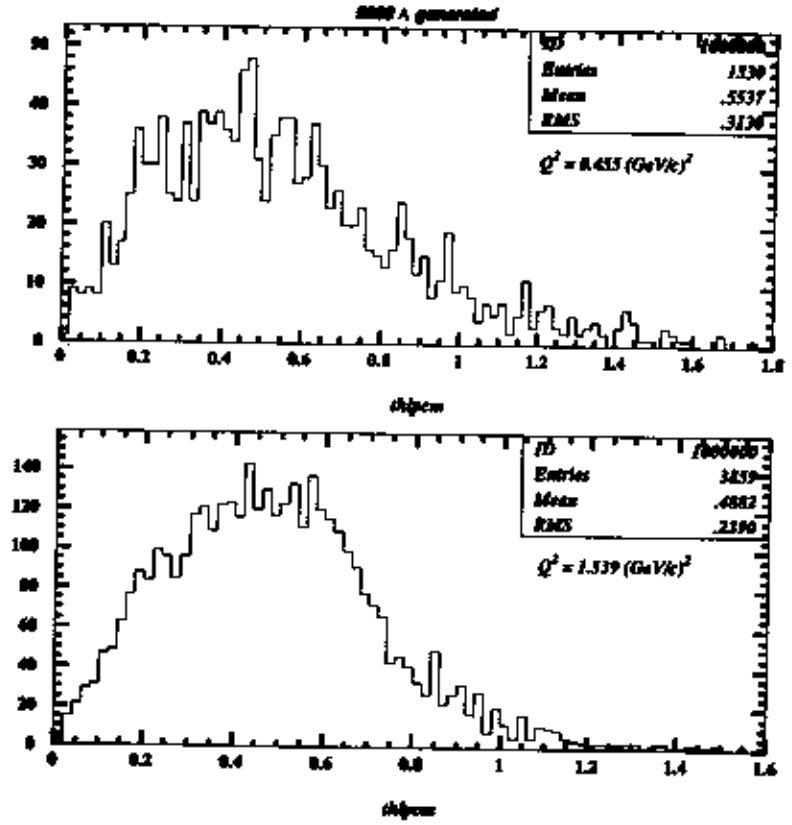

Figure (13). The Monte Carlo simulation of the distribution of the angle between the hyperon and the decay proton at two momentum transfer settings.

For each successful two-track event in the SOS, the energy and momentum of the missing particle (the pion) is reconstructed. Afterwards, a weight is applied corresponding to the model of Williams [23]. Depending on the kinematic setting, the angle between the proton and the Λ is allowed to vary by up to 10° in the lab

frame. This is due to the fact that it is not necessary for the hyperon to fall within the SOS acceptance, but rather that the decay-proton momentum and angle lie within the spectrometer acceptance. Simulations at 0.455 and 1.545 GeV^2/c^2 are presented. Simulations have been carried out for all of the proposed kinematic settings as recommended by PAC-12.

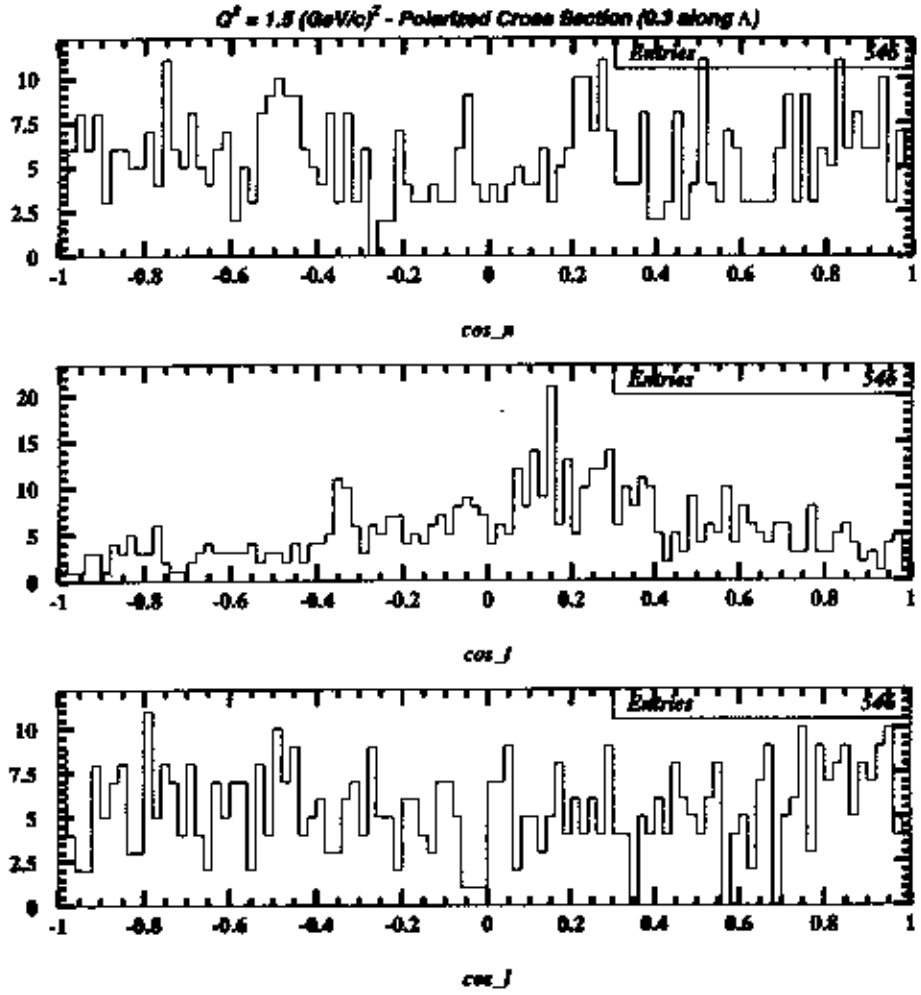

Figure (14). The simulated proton angular distribution (in the hyperon rest frame) along the three spin directions (see Fig. (1)) for a 30% hyperon

polarization at Q^2 of 1.5 $(GeV/c)^2$.

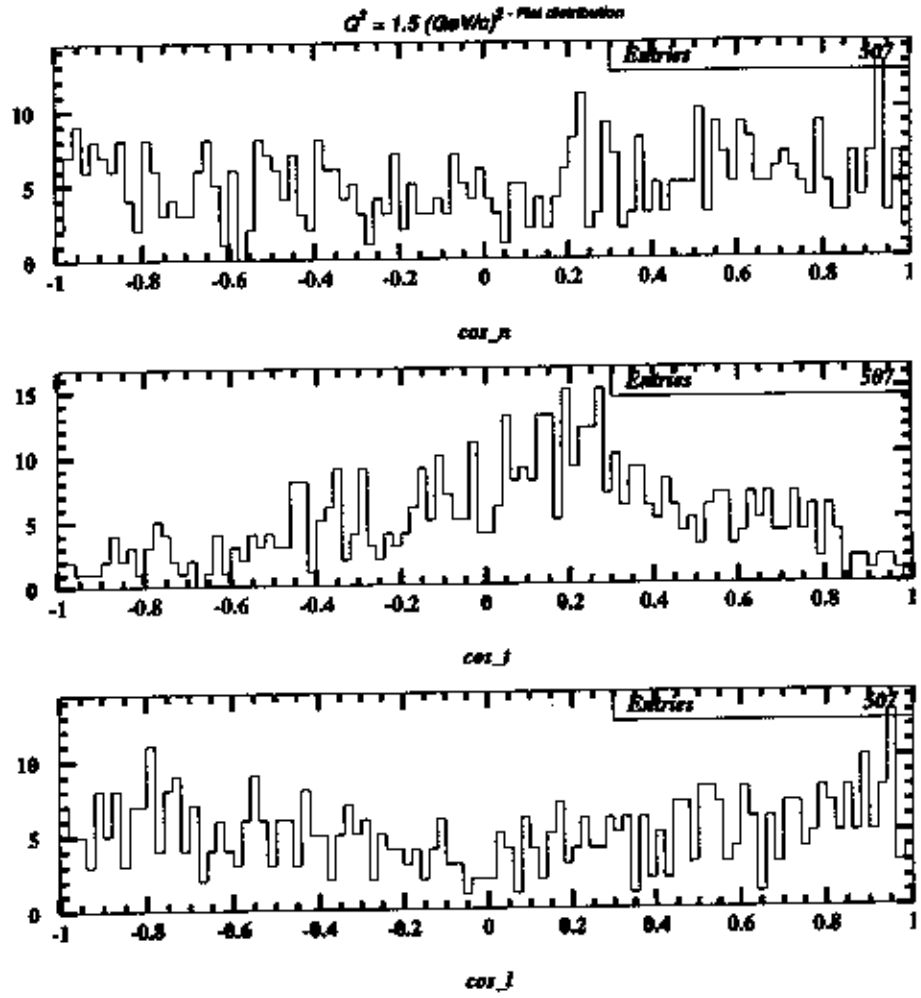

Figure (15). The simulated proton angular distribution (in the hyperon rest frame) along the three spin directions (see Fig. (1)) for a flat cross section and no hyperon polarization. The simulation is for Q^2 of 1.5 $(GeV/c)^2$.

Shown in Fig. (12) is a comparison of the pion missing mass at the two momentum transfer points, 0.46 and 1.54 $(Gev/c)^2$. For a given number of hyperons generated in both cases (5000 total), more protons are detected which reconstruct the pion missing mass at the higher Q^2 setting as expected. This is due to the forward focussing at the higher momentum transfer. Fig. (13) shows the

angle between the decay-proton and the hyperon momentum direction in the center-of-mass system (cms) for the two Q^2 settings. The angular range is the same in the cms, however the number of events which reconstruct a pion missing mass is greater at the higher Q^2 point.

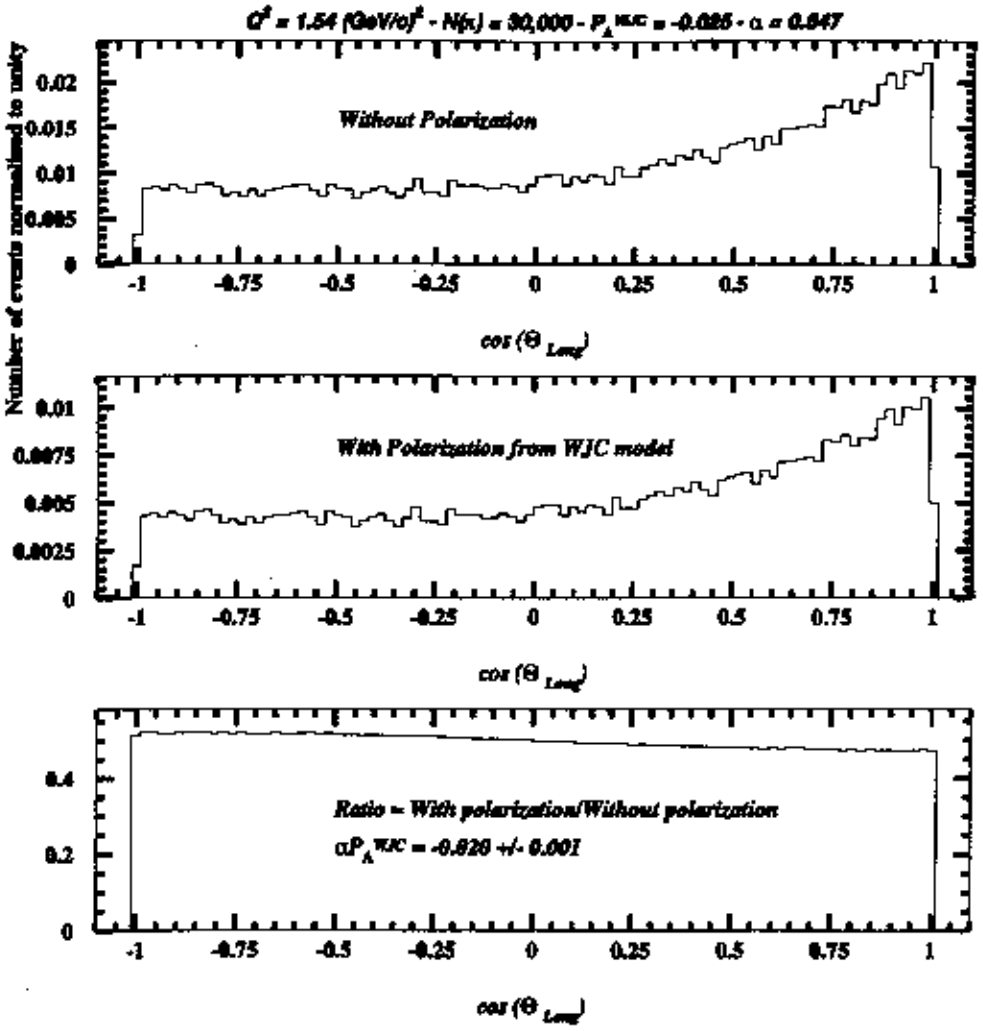

Figure (16). The ratio r of the polarized to unpolarized Λ-decay proton angular distribution versus the cosine of the angle between the hyperon spin axis and the proton momentum vector. The hyperon polarization along its momentum direction is simulated to be 0.25 at Q^2=1.5 $(GeV/c)^2$.

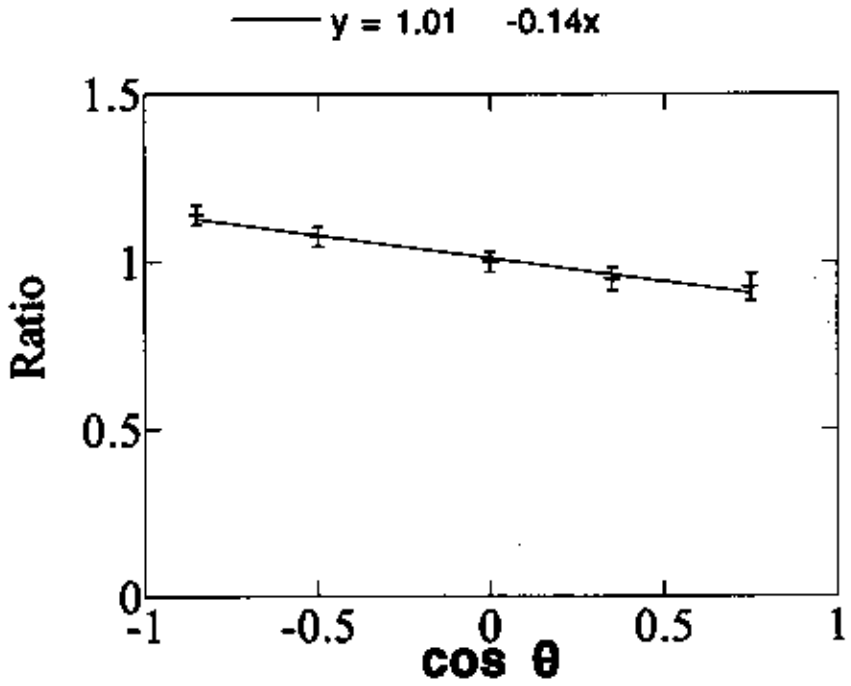

Figure (17). The straight line fit to the ratio of polarized to unpolarized distribution of Λ-decay protons is used to extract the hyperon polarization as shown.

One of the questions to be answered by this Monte Carlo simulation is whether a reasonable hyperon polarization can be measured with the Hall C apparatus. A 25% hyperon polarization was assigned on the simulation input and events generated as described above. The simulation results are shown in Fig. (14). The results were compared with the distribution obtained from a flat cross section and no polarization. This is shown in Fig. (15). This distribution from a flat cross section and no polarization is used to determine the shape of the acceptance which will be used to extract the corrected angular distribution of hyperon-decay-protons. The decay-proton spectrum was analyzed to extract the polarization using (8).

In the experiment, for the decay proton angular distribution, both the distribution with an unpolarized beam as well as with a polarized beam will be determined.

Experimental Uncertainty Analysis

Let r be the ratio of the polarized proton distribution to the unpolarized distribution for a given bin in the cosine of the angle between the hyperon spin direction and the proton momentum direction as shown in Fig. (16).

$$r(\cos\theta) = N^{pol}(\cos\theta)/N^{unpol}(\cos\theta) \qquad \text{(EQ 11)}$$

The r versus $\cos\theta$ will yield a straight line with slope equal to αP, where P is the hyperon polarization and $\alpha = 0.642$. This will be done for all three of the hyperon spin axes. The error on the slope can be extracted as follows: Let the equation of the best line through the data of R versus $\cos\theta$ be

$$r = m(\cos\theta) + b \qquad \text{(EQ 12)}$$

where $m = \alpha P$. The value for the standard deviation of the slope, δm is calculated from

$$\delta m = \delta r \sqrt{\frac{N}{N\sum \cos\theta_i^2 - (\sum \cos\theta_i)^2}} \qquad \text{(EQ 13)}$$

with the standard deviation of the distribution of δr values about the best fit line given by

$$\delta r = \sqrt{\frac{\sum (\Delta r_i)^2}{N-2}} \qquad \text{(EQ 14)}$$

and

$$\Delta r_i = r_i - (m\cos\theta_i + b) \qquad \text{(EQ 15)}$$

Here N is the total number of counts in the $\cos\theta_i$ bin as shown in Fig. 16. A straight line fit to the ratio of polarized to unpolarized distribution as a function of $\cos\theta_{psA}$ yields the slope as proportional to the hyperon polarization as shown in Fig. (17). The slope of the least squares fit to the simulated data is 0.26 +/- 0.03 as shown. The error is statistical only with 2.7% overall statistics. Thus the value extracted from the analysis agrees well with the input hyperon polarization. This

technique has been simulated and tested for polarization along all three hyperon spin axes and for hyperon polarization parallel and anti-parallel to the three spin axes x', y', and z'. This ensures that one can cross-check the hyperon polarization by flipping the electron helicity and hence the hyperon spin direction. This was a recommendation from PAC-12. The ratio of integrated events under the peaks of the kaon and pion in the missing mass spectra give an estimate of the number of protons from Λ decay that can be expected in the experiment. (The proton in this case is used to identify the $\vec{\Lambda}$ spin polarization vector.) The results of the Monte Carlo simulation indicates that on average, about 5% of the kaons (for unpolarized Λ-hyperons) which give reconstructed Λ-hyperons yield an identified π^--meson. These results were first obtained by B. Mecking using a separate Monte Carlo simulation with measured HMS and SOS acceptances [28]. These results was used in estimating the required measurement time for each data point.

The SOS as a Hyperon Tagger: Data from E93018

The procedure proposed for data analysis has been tested on a subset of the data from E93-018, recently completed in Hall C. For one series of measurements at Q^2=1.5 $(GeV/c)^2$, the kaons and hyperons were both produced at forward angles (in the laboratory system) with respect to $\vec{q}$ and with the same laboratory momenta. The scattered electrons were detected in the HMS while the kaons were detected in the SOS before their decay in flight. The particle identification for the reaction shows clearly the kaons from the reaction. (See Figs. (7) and (8)). For these momenta, a clear Λ peak in the missing mass spectrum is seen (see Fig. (9)). In some fraction of these coincident events, a second particle with the velocity identified with that of a proton, was detected in the SOS, in coincidence with the kaon. From the measured energy and momentum of the scattered electron, kaon, and coincident proton, a missing mass (mass of X) of the process

$$e + p \rightarrow e' + K + p + X \qquad \text{(EQ 16)}$$

was determined, indicating that the particle was a pion from the decay

$$\Lambda \rightarrow p + \pi \qquad \text{(EQ 17)}$$

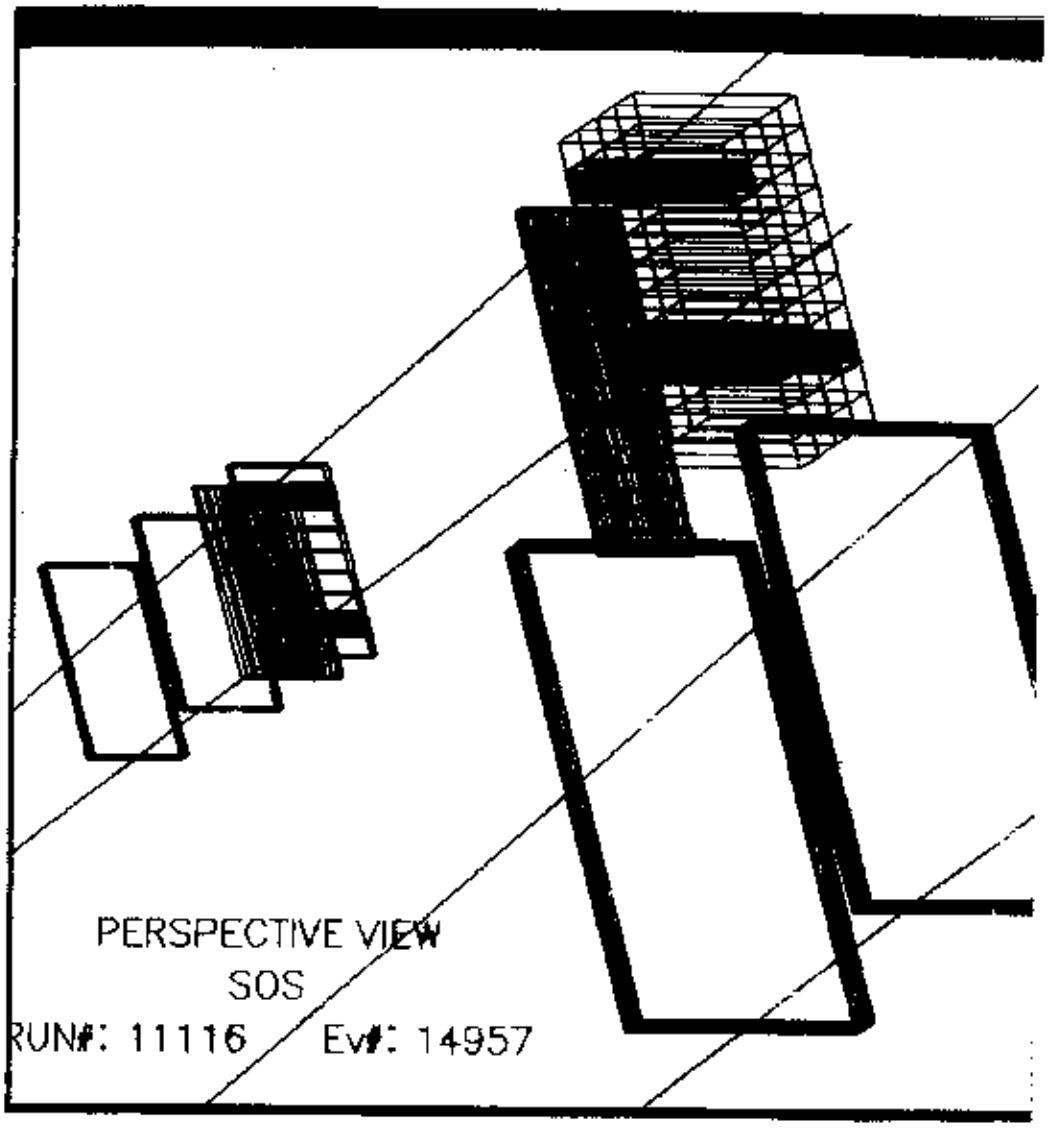

Figure (18a). The single event display of an event (taken during E93018) in the SOS detector stack with two fully reconstructed particle tracks. The SOS will be used to identify kaons as well as protons (from hyperon decays) in the same event.

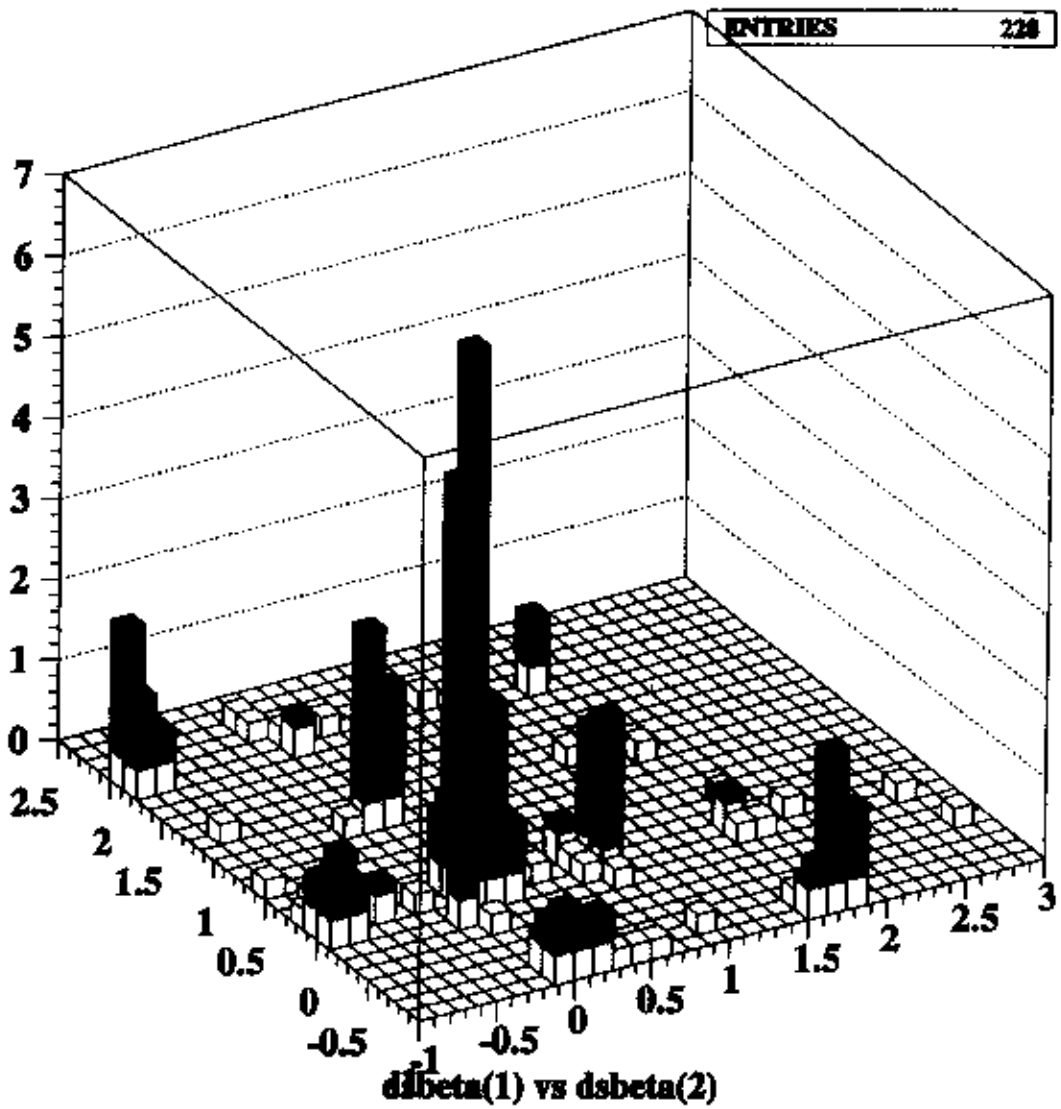

Figure (18b). Particle identification via time-of-flight is used to determine that one of the particles of this one event is a kaon and the other is a proton from the hyperon decay. The data shown in this figure is from E93018.

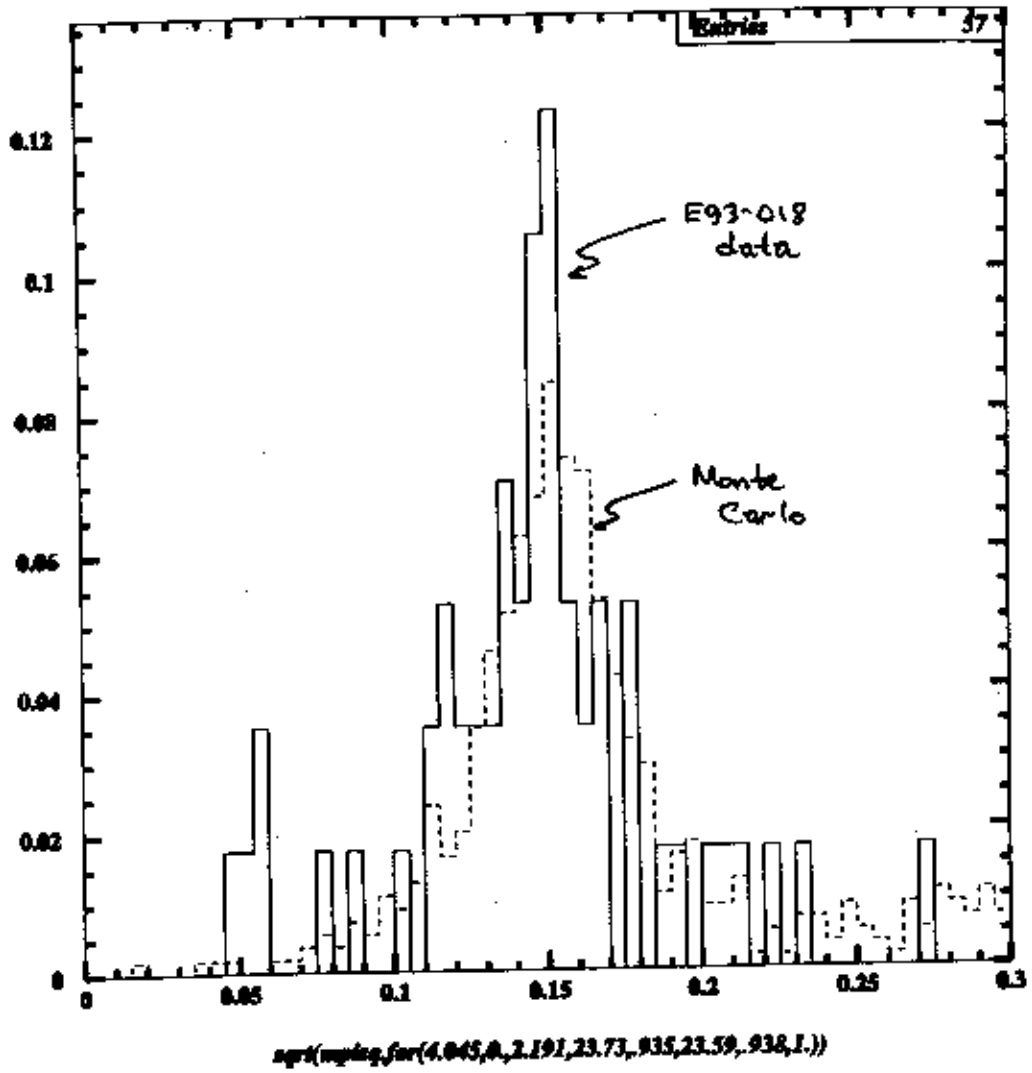

Figure (18c). The calculated missing mass using the information from the two-track events shown above indicates that the reaction is given by (3), only with no polarization observed. The missing mass of the pion from the Λ decay is clearly visible. The data is from E93-018. The dashed line in the Monte Carlo simulation of the events.

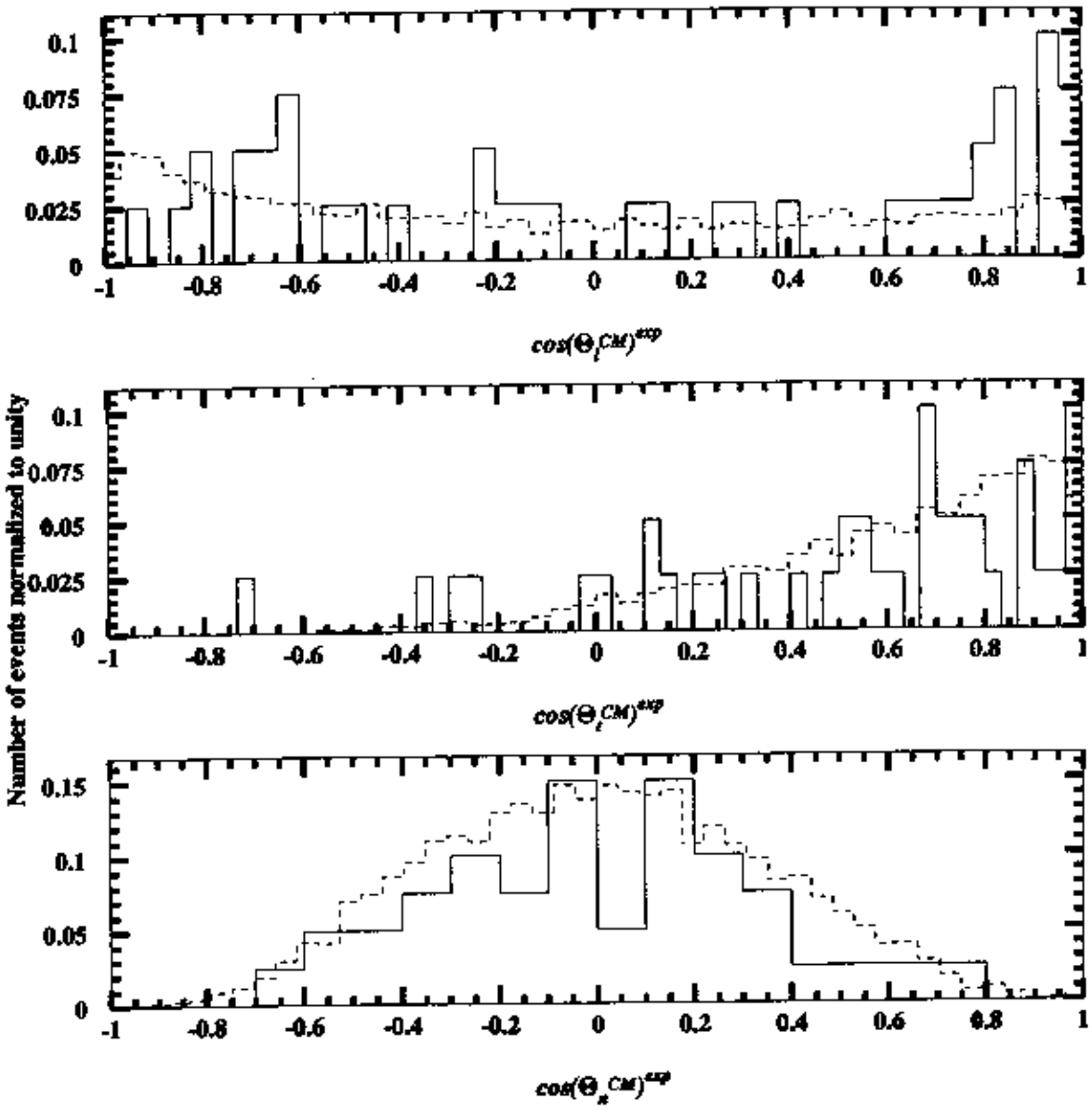

Figure (19). The projection along the three hyperon spin axes: (a) along z (b) along x and (c) along y as defined in Fig. 1 for the data from E93-018.

The single event display for the SOS detector stack is shown in Fig. (18a) for an event where two particles were detected within the same coincidence window. For this event, the velocity (β) of particle 1 (2) is 0.83 (0.64). See Fig. 18b. From the SOS momentum setting the particle is identified as a kaon (proton). The pion in the corresponding missing mass calculation indicates that the analysis

procedure works (Fig. 18c). Hence, this analysis procedure can be used to identify the Λ decay products from the kaon electroproduction event (the hyperons are determined from missing mass in the standard way). This technique will be applied for all of the kinematic points measured in this experiment. The projection along the three hyperon spin axes shown in Fig. (1) for the E93018 data are presented in Fig. (19).

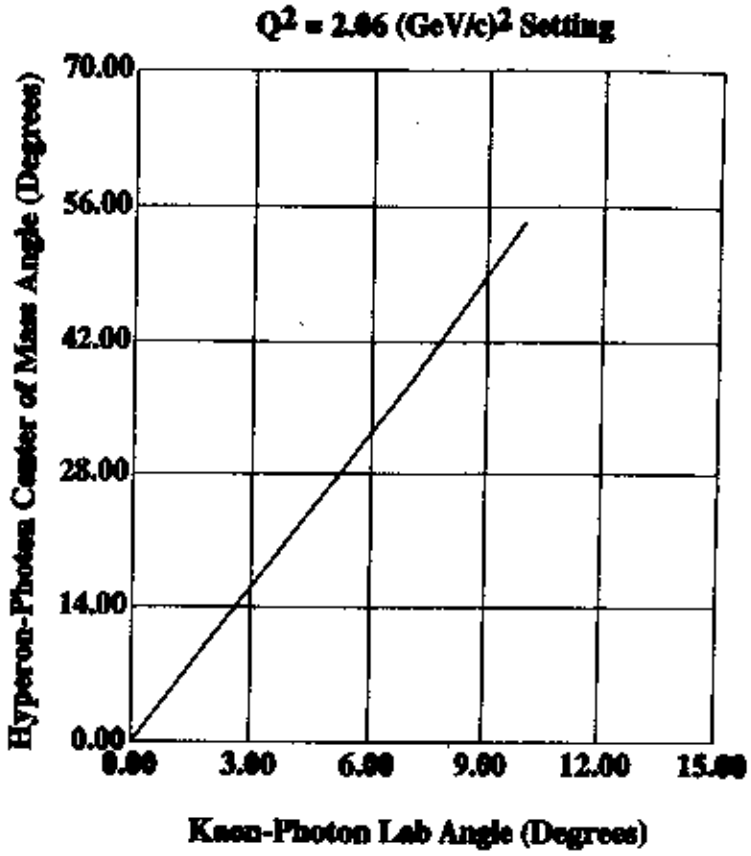

Figure (20). The angular acceptance in the SOS for hyperons with respect to the virtual photon versus kaon - photon lab angle. The SOS has roughly a 5 degree full angular acceptance.

The effect of the finite SOS (polar) angular acceptance is shown in Fig. (20). Plotted is the Λ-hyperon angle with respect to the virtual photon, in both the lab frame and the center of mass frame, versus the kaon - photon lab angle. The SOS angular acceptance is about 5 degrees corresponding to a maximum hyperon - photon angle of just under 30° in the center of mass. The kaon and hyperon momenta in the experiment for a representative set of kinematics is shown in Fig. (21) for the finite HMS (electron arm) acceptance. Again, the kaon and hyperon

momenta must be roughly equal in order for the SOS to be used as a hyperon tagger in the manner proposed. The rather large momentum acceptance in the SOS as indicated in the figure, permits kaons and protons from hyperon decay to be detected over a large momentum range.

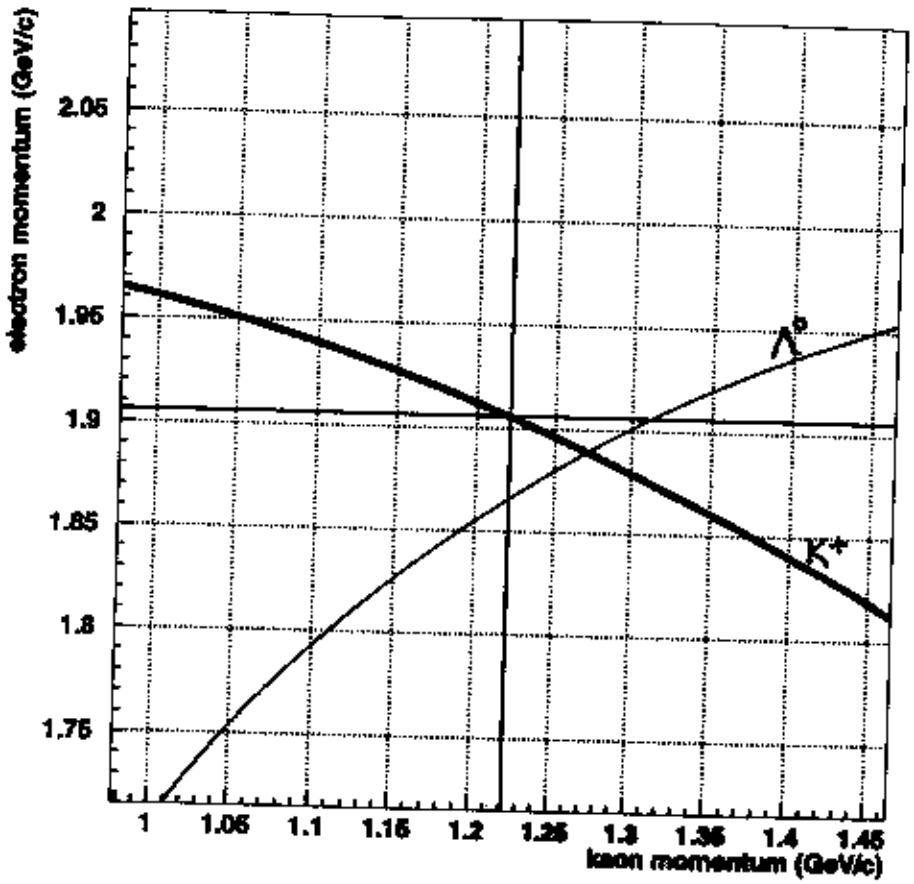

Figure (21). The momentum range in both the SOS and HMS for a representative kinematic setting of the experiment. The large SOS momentum acceptance gives flexibility in detecting both the kaon and the proton from the hyperon decay. The SOS has a 5 degree angular acceptance.

Expected Corrections

Previous work in p(e,e'K^+) experiments indicate that the detector stack will give uncertainties associated with each detector element as corrections are applied to the detectors. The corrections will be determined by Monte Carlo simulations and during the actual experiment. The expected uncertainties associated with the corrections are listed as follows:

TABLE 2. Expected Errors on Corrections

Counter Dead Time	**1.5%**
Wire Chamber Inefficiencies	**0.5%**
Electron Shower Counter Inefficiencies	**1.0%**
Kaon Absorption in target/detectors	**1.0%**
Kaon Arm Cherenkov-Counter Inefficiencies	**2.0%**
Kaon Decay	**3.0%**
Knock-on Events Firing Cherenkov	**1.0%**
Target Wall Events	**0.5%**
Randoms	**1.0%**
In Time Kaon Losses	**1.0%**
Radiative Corrections (Photon Radiations)	**3.0%**
Acceptance Correction	**2.0%**
Beam Polarization (80\% polarization)	**1.0%**
Quadratic Sum	**6.0%**

Note that this is 6% of the corrections which are expected to be about 30 - 70%. The total systematic uncertainty due to the above corrections is expected to be about 4-5%.

The hyperon polarization in the polarization transfer measurement (3) will be determined to approximately 8%. Then the polarization transfer coefficient $R_{TT'}^{x'0}$ and $R_{TL'}^{x'0}$ will be determined (from equation (7)) to 10-12%.

Rates and Beam Time Request

The singles rates, R, in each of the spectrometers separately was obtained from the results of experiment E93-018 which are consistent with

$$R = n_i \cdot n_t \cdot t \cdot \frac{d\sigma}{d\Omega} \cdot \Delta\Omega \cdot (1 - P_{decay}) \qquad \text{(EQ 18)}$$

where n_i is the number of incident particles per second on a target of thickness t and target density n_t. $d\sigma/d\Omega$ is the scattering cross section and $\Delta\Omega$ is the spectrometer solid angle. The count rate is corrected for kaon survival probability.

In the electron arm, the singles rates were measured to be below 10 kHz when using a 35 μA beam and the 4-cm target and with the HMS at a forward angle. This is well below the design limit for the detectors in the spectrometer detector stack. In the hadron arm, the singles rates are kept below 1 MHz with 35 μA beam current. Again, this is adequate for the experiment.

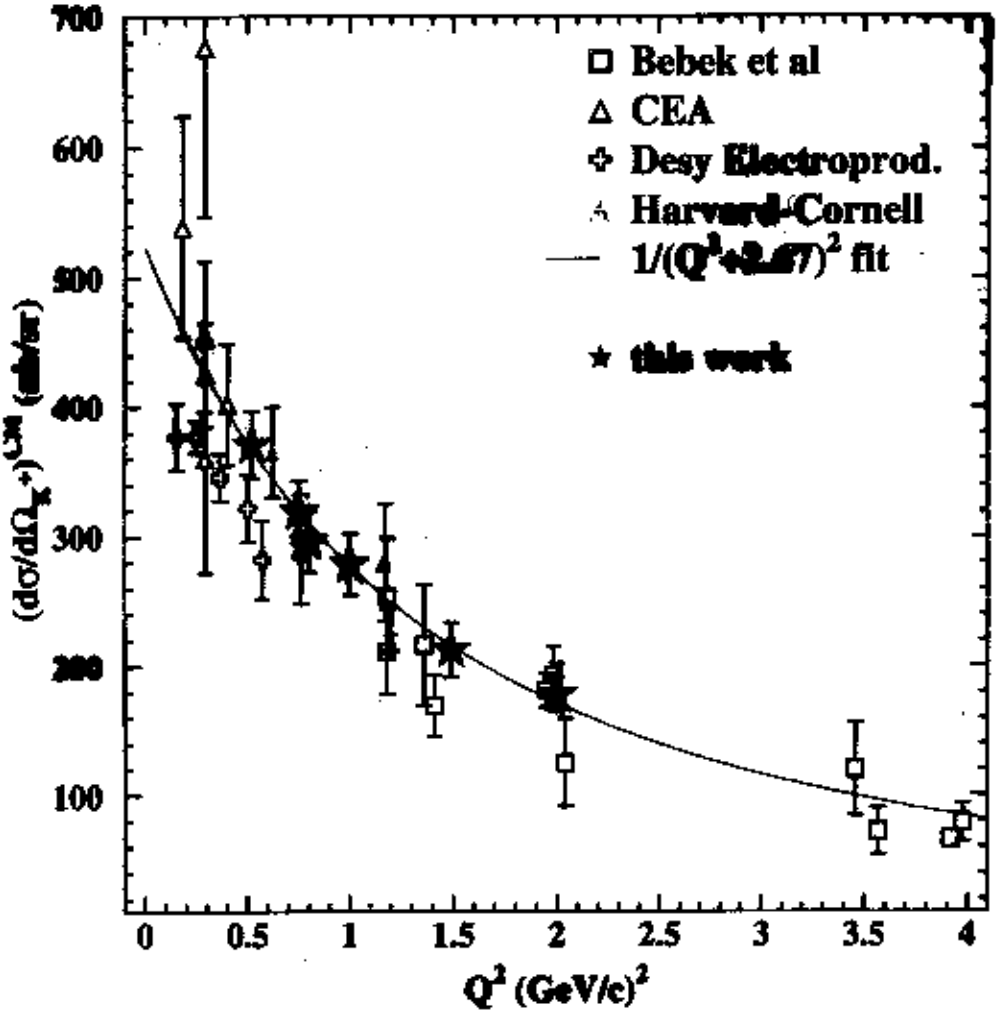

Figure 22. The center of mass cross section for the reaction e + p ---> e' + K^+ + Λ (from reference [29]).

The coincidence rate, R_{coin}, for the HMS and SOS used in this experiment is known from the results of the Hall C kaon electroproduction experiments (using an unpolarized electron beam). The center of mass cross section from Experiment E93-018 is shown in Fig. 22. The cross section is extracted using the formula:

$$R_{coin} = \frac{i}{e} \cdot \frac{\rho t N_o}{A} \cdot \varepsilon_D \cdot \frac{d^3\sigma}{dE_{e'} d\Omega_{e'} d\Omega_K} \cdot \Delta E_{e'} \cdot \Delta\Omega_{e'} \cdot \Delta\Omega_K \cdot (1 - P_{dec}) \qquad \text{(EQ 19)}$$

Here $\Delta\Omega$ is the solid angle of the spectrometer, ε_D is the detection efficiency, i is the beam current, N_o is Avogadro's number, e is the electron charge, t is the target thickness of mass number A and density ρ. For the HMS spectrometer, $\Delta E / E$ will be about 20%. The cross section using a polarized electron beam will be measured similarly.

An estimate of the number of accidental to true coincidences A/T is obtained from

$$\frac{A}{T} = \frac{\tau \cdot R_e \cdot R_K}{R_{coin} \cdot f} \qquad \text{(EQ 20)}$$

where the duty factor f is 100% for the CEBAF machine and the resolving time, τ, is taken to be 1.0 ns offline and 30 ns online. The E93-018 data indicates that the accidental rates even for a 40 μA beam is reasonable for the proton target and the detector configuration proposed in this experiment. Although A/T could be reduced somewhat by lowering the beam current (at the expense of counting rates), this ratio should allow a 3% (statistical) measurement without difficulty. Currently, in the analysis of the E93-018 data, A/T ratios of 1/50 are reasonable offline.

TABLE 3. Beam Time Request

Data Acquisition	**13.0 days**
Setup and Checkout	**1.5 days**
Background Studies	**1.0 days**
Angle and Momentum Changes	**0.5 days**
TOTAL	**16.0 days**

A measurement at the momentum transfers proposed here with the statistics

required will require approximately 16.0 days of beam time, including setup time. This is summarized in the table above.

The Collaboration

The collaboration will include institutions and personnel that have made substantial contributions to building hardware and readying software for the experiment. Additionally, most of these collaborators will have taken part in the initial kaon electroproduction experiments (E91-016 and E93-018) in Hall C during the fall of 1996. Graduate students will use this experiment as part of their dissertation research. The Hampton University group has 6 graduate students, 3 postdocs and 3 (presently) faculty members involved in experimental work, and 3 faculty, 1 postdoc, and several students providing theoretical support. Other institutions provide similar levels of effort as part of this collaboration.

Response to Specific Issues Raised by PAC-12

This proposal is based upon a previously-submitted proposal, PR-97-007 which as conditionally approved by PAC-12 in 1997. There were three specific issues raised by PAC-12 which we have addressed in this Proposal.

- *An extensive simulation of the experiment.* We have developed and run an extensive Monte Carlo simulation of the experiment for all of the kinematic settings of Tables 1 and 2. Some of the results are included in this manuscript. Many more results are available upon request.
- *Check whether the spectrometer acceptances allow the polarization to be measured.* We have verified this with the Monte Carlo simulation for all of the kinematic settings.
- *Cross-check of hyperon polarization measurement by flipping electron helicity.* The helicity-dependent hyperon polarization can be checked by flipping the electron helicity as verified by our Monte Carlo simulation. The helicity-independent polarization can be cross-checked by measuring kaons both left and right of the momentum transfer vector.

References

1. J. D. Walecka, Argonne National Lab. Report ANL-83-50 (1983).
2. S. Nozawa and T. S. Lee, Nucl. Phys. A513, 511 (1990).
3. W. E. Kleppinger and J. D. Walecka, Ann. Phys. 146, 349 (1983).
4. T. De Forest, Jr., Ann. Phys. 45, 365 (1967).
5. G. Gourdin, IL Nuovo Cim. 221, 1094 (1961).
6. D. R. Yennie et. al., Rev. Mod. Phys. 29, 144 (1957).
7. G. Knochlein et. al., Z. Phys A352, 327 (1995).
8. R.A. Adelseck and B. Saghai, Phys. Rev. C42, 108 (1990).
9. R. Schumacher (Spokesperson), Jefferson Lab Experiment E89-004 (1989).
10. A. Bravar et. al., Preprint FermiLab-Pub-96/393-E E704 (1997).
11. M. Burdart and R.L. Jaffe, Phys. Rev. Lett. 70, 2537 (1993);X. Artru and M. Mekhfi, & Nucl. Phys. A532, 351c (1991).
12. See for example R. K. Bhaduri, **Models of the Nucleon**, Addison-Wesley Publ. Co., Menlo Park, CA (1988).
13. J.M. Finn and P.A. Souder et. al., CEBAF PR 91-010.
14. D. Beck et. al., CEBAF PR 91-017.
15. L.L. Foldy, Phys. Rev. 83, 688 (1955).
16. L.L. Foldy, Rev. Mod. Phys. 30, 471 (1958).
17. R.G. Arnold et al., Phys. Rev. Lett. 57, 174 (1986).
18. C. Bennhold, Phys. Rev C 43, 775 (1991).
19. R. Hofstadter et al., Rev. Mod. Phys. 30, 482 (1958); R. Hofstadter et al., Phys. Rev. 98, 217 (1955).
20. NSAC Report (1989).
21. M.I. Adamovich et al., Z. Phys. A350, 379 (1995).
22. B. Krusche et al., Phys. Rev. Lett (1996).
23. R. W. Williams, Ph. D. Dissertation, NCSU (1993) and private communication (1997).
24. C. Bennhold and T. Mart, private communications (1997).

25. Jefferson Lab Experiment E93-018, O.K. Baker spokesman (1996).

26. N. Makins, Ph.D. Dissertation, MIT (1994).

27. P. Gueye, private communications, (1995).

28. B. Mecking, private communications (1996).

29. G. Niculescu et. al. submitted to Phy. Rev. Lett. (1998).

Polarization Transfer in Kaon Electroproduction:

Collaboration

K. Assamagan, O.K. Baker (Spokesman)[†], P. Gueye, C. Keppel, R. Madey, L. Tang[†], R. Williams
Hampton University, USA
[†]and, jointly, Thomas Jefferson National Accelerator Facility, USA

J. Dunne, R. Ent
Thomas Jefferson National Accelerator Facility, USA

C. Bennhold, K. Dhuga, T. Mart
George Washington University, USA

M. Eckhause, D. Hancock, J. Kane, Y. Kuang, B. Welsh
College of William and Mary, USA

C.C. Chang
University of Maryland, USA

P. Markowitz
Florida International University

J. Reinhold, B. Zeidman
Argonne National Laboratory, USA

S. Beedoe, S. Danagoulian, C. Jackson, S. Mtingwa, R. Sawafta
North Carolina A&T State University, USA

E. Cisbani, S. Frullani, F. Garibaldi, M. Iodice, G.M. Urciuoli
INFN, Rome

T. Saito
Tohoku University, Japan

W. Kim, P. Kim
Kyungpook National University, South Korea

Kyungseon Joo
University of Virginia, USA

T. Angelescu, L. Teodorescu
Bucharest University, Romania